5-2017

Ab Initio and Semi-Empirical Calculations of Cyanoligated Rhodium Dimer Complexs

Yazeed Asiri
East Tennessee State University

Ab Initio and Semi-Empirical Calculations of Cyanoligated Rhodium Dimer Complexes

A thesis

presented to

the faculty of the Department of Chemistry

East Tennessee State University

In partial fulfillment of

the requirements for the degree

Master of Science in Chemistry

by

Yazeed Asiri

May 2017

Dr. Scott Kirkby, Chair

Dr. Marina Roginskaya

Dr. David Close

Keywords: *Ab Initio* Calculations, Hartree-Fock Self Consistent Field, Density Functional Theory, Dirhodium Complexes, Atomic Units

ABSTRACT

Ab Initio and Semi-Empirical Calculations of Cyanoligated Rhodium Dimer Complexes

by

Yazeed Asiri

Molecular modeling, using both *ab initio* and semi-empirical methods has been undertaken for a series of dirhodium complexes in order to improve the understanding of the nature of the chemical bonding in this class of homogeneous catalysts. These complexes, with carboxylamidate and carboxylate ligands, are extremely functional metal catalysts used in the synthesis of pharmaceuticals and agrochemicals. The X-ray crystallography shows anomalies in the bond angles that have potential impact on understanding the catalysis. To resolve these issues, minimum energy structures of several examples (e.g. $Rh_2(NHCOCH_3)_4$, $Rh_2(NHCOCH_3)_4NC$, $Rh_2(CO_2CH_3)_4$, $Rh_2(CO_2CH_3)_4NC$, $Rh_2(CHO_2)_4$, and $Rh_2(CHO_2)_4NC$) were calculated using Hatree-Fock and Density Functional Theory/B3LYP with the LANL2DZ ECP (Rh), and cc-pVDZ (all other atoms) basis sets.

DEDICATION

I dedicate this project to the Almighty God, my mother, my wife, and Mr. Mohammed Alwehaibi. This work is also dedicated to the memory of my father.

ACKNOWLEDGMENTS

This work would not have been possible without the help and support of so many people. First, I am thankful to God for His guidance and protection. I thank my supervisor, Dr. Scott Kirkby, for his persistent and professional advice throughout my graduate studies at East Tennessee State University (ETSU). I express my deep sense of gratitude to Dr. Marina Roginskaya and Dr. David Close for accepting to serve on my committee. I am very much thankful to Dr. Cassandra T Eagle, and her research group. I acknowledge with thanks the kind of love and support, which I have received from the faculty and staff of the Department of Chemistry at ETSU.

I wish to express my sincere thanks to my family, specially my mother, who believed in me. I also thank my wife for her emotional support and honesty over these years. I thank all the past and present graduate students in the Chemistry department.

TABLE OF CONTENTS

LIST OF TABLES

LIST OF FIGURES

Figure Page

CHAPTER 1

INTRODUCTION

Computational techniques in advanced chemistry mimic atomistic systems to study their behavior and properties mathematically.[1] It is a theoretical approach of simplifying graphical models that has long inspired the molecular graphics in published works, books and, more recently, on computers. In other words, molecular modeling has revolutionized the understanding of chemistry visually and quantitatively.[2] It consequently leads to the process of generating and testing hypotheses. In the past, prediction of a chemical reaction's outcomes and molecular designing required a specialist, but today, high performance digital computers offer advanced graphic and computing tools that facilitate students in theoretical chemistry to perform calculations of molecular reactions as well as conformational analyses interactively on their desktop computers in any college or industry.[1-4]

Molecular modeling is used as a computational tool for interpreting, elucidating, and investigating existing and novel phenomena in several areas of chemistry such as molecular structure determination by NMR spectroscopy, catalysis, biometrics, protein mutagenesis, and nucleotides/ protein interaction studies.[5,6] It has changed the face of pharmaceuticals by contributing in drug design studies and, consequently, creating incredible opportunities for advanced therapeutic research in the studies of drug-drug as well as drug-living organism interactions at the molecular level.[2]

Efficacy of the Molecular Modeling

Molecular modeling is a way of reinterpreting the molecular orbitals. Therefore, this approach has become the preferred choice of many chemists for varied applications in several

areas of the chemistry. Moreover, these tools are in practice in several empirical research studies.[4] In his research paper, Robert D. Hancock carried out molecular mechanics calculations to compare the size of a chelate ring with that of the macrocyclic ring in a metal ion.[7] He reasoned out his selection of this approach as molecular mechanics calculations are easy-to-solve calculations for modeling molecular steric effects in a coordinate compound. The approach provides simple equations to analyze the steric strain, such as the length and angle of a deformed bond, torsional strain, and non-ionic interactions like van der Waals forces.[7] In a study on metal complexes conducted by Sun *et al*., relative stability and behavior of two metal complexes-gallium (III) and indium (III) complexes with bis(aminoethanethiol) ligands were investigated,[8] and the parameters of the force fields for bonds between the donor atoms (N, O, and S) with both metals were obtained as structural data from the Cambridge Structural Databank, for a modeling package SYBYL (commercially available).[9] In several projects, molecular modeling was used to validate the correlation of a metal ion size with a ligand selectivity by studying the energetics of the metal-ligand (M-L) bond length, expressed mathematically as the complex strain energy. To serve this purpose, they successfully modeled the complex-ligated metal.[7,10-12]

A significant feature of molecular modeling methods is that they enable synthetic chemists to design effectively, the substrates and catalysts-ligands scaffolds to predict the high-yield or to predict the selectivity and reactivity. This important attribute of molecular modeling was exploited by Xufeng and coworkers[13] to examine and interpret the structure and the energetics of four reaction pathways catalyzed by dirhodium tetracarboxylate in the amidation-aziridation chemical reactions at the intra-molecular level, by Density Functional Theory (DFT) calculations. They used the 6-311G* basis set for all non-transition elements: C, O, H, S, N, and I atoms in this experiment. Further, they refrain themselves from using all-electron basis set in

case of Rh atom and instead opted for using the Effective Core Potential (ECP) basis such as LANL2DZ, a popular approach in transition metals computation.[13] Similarly, Li and coworkers[14] used DFT and similar basis sets as discussed before, in the context of the pyrene-armed calyx [4] azacrowns undergoing a "Molecular Taekanwando." The process was optimized, and the frequency of harmonic vibrations were calculated at the B3LYP/6-31G(d) level of theory and employing the effective-core potentials, the LANL2DZ, for the heavy cesium and silver metal ions.

In this process, HF and the hybrid exchange correlation functional (HF-DFT functional) were used to attain the geometry optimization and to calculate single point energy. LANL2DZ ECP basis set was applied for the rhodium atom while 6-31G basis set was used for all the other atoms. HF and DFT are commonly used methods to perform calculations in quantum chemistry. The main reason for using these two methods is mostly to compare between the results obtained in both methods.

When spatial basis functions were introduced in the 1950s, such as Roothan-Hall equations[15-16] and/or Gaussian-type[17], the emerging computing science adopted the Hartee-Fock (HF) method. The HF method gives approximate solutions for effective bond lengths after optimization.[18] It is a widely applied method, the approximation solution is taken as a reference wavefunction for advanced calculation methods like Coupled-Cluster calculations and Møller-Plesset perturbation theory.[4]

Similarly, the DFT method is widely applied alongside the closely related HF method, but DFT is a comparatively more accurate method because it produces reliable results and it measures accurately the computed structures and relative energies of the molecules.[19] Since the DFT method tends to account minimally for electron correlation, its accuracy lies in between the

accuracies of HF and MP2. It can be best studied in the application of B3LYP, a hybrid functional, into the studies of the complexes of transition metal atoms[19] such as dirhodium systems that yields accurate results in relation to atomization energies and frequencies as well as optimum geometry.[20] Generally, the net and the relative computing time used for performing calculations by DFT and HF method is determined by variables such as the size of the concerned system, the hardware and the software components of the computer used.

The various approximation of Schrödinger equation is demonstrated by the coupling of HF with a basis set, and the paring of B3LYP with a basis set. Moreover, expanding the basis set usually yields more precision. Thus, bigger basis sets give a better orbitals approximation by requiring less restrictions on the electrons locations in space. Although this model guarantees more accuracy, the pairing of a large basis set with more reliable methods leads to a time-consuming process at greater computational expenses. Therefore, in lieu of the stated considerations, a suitably large 6-31G* basis set was selected for the systems under study.

Dirhodium Complexes

Dirhodium compounds and the bridging ligands in their complexes, is an emerging catalysts class that is effective in diverse reactions and their efficiency is attributed to their structural hardness, ligand exchange activity, their diaxial sites available for coordination with Lewis bases, and low oxidation potentials such as (0.011V) in dirhodium(II) caprolactamate, and (1.17V) in dirhodium (II) carboxylates.[21] In this class, complexes with carboxamidate ligands have the broadest applications in organic chemistry.[21]

Redesigning the dirhodium core via ligand exchange modifies the selectivity of the catalyst. The nature of the ligand bridge alters the electronic properties of the metal, which

reproduces a changed catalytic behavior. For example, substitution of the acetate ligands with any of the carboxyamidates, amidinates, and thio-carboxylates in a dirhodium catalyst increases the electron density around the rhodium centers. A study was done on the catalysis of the dirhodium carboxyamate complexes to examine how the steric balance around the active site of the catalysts improves their stereoselectivity and reactivity.[22]

Several reports are available as published works and studies on the rhodium acetate complex and the utility of these complexes.[23] The best studied complex is $M_2(O_2CR)_4L_n$ (where n=1 or 2; L = axial ligand).[23] Ligation of acetate ion to the complex results in single dirhodium isomer whereas ligation of acetamide yields four isomers, labeled as *2,2-cis, 2,2-trans, 3,1-trans,* and *4,0-trans*- prefixes to the central part of the complexes. Figure 1 depicts the bond arrangements in these molecules.[24]

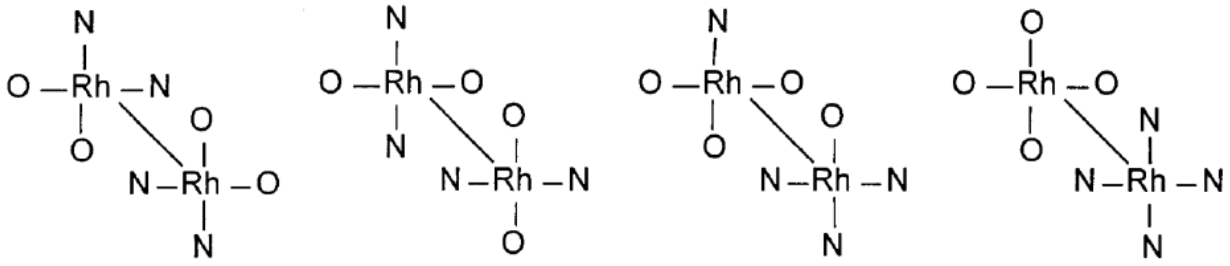

Figure 1: Diagram of the central bonding arrangement for the isomeric structures of tetrakis (carboxylamidate) dirhodium (II).

Complex Formation

In transition elements, d-orbitals can form a maximum of four bonds as is evident in the case of the quadruple bonding of chromium and rhodium in their complexes.[24] When two atoms approach each other, their symmetry properties allows only five non-zero overlapping between set of orbitals. Rhodium-carbene bond uses both δ bonding and π back bonding, wherein the combination creates a stable but short-lived bond.[25]

The positive overlap of the two d_z^2 orbitals: $d_z^{2(1)} + d_z^{2(2)}$ yields a δ bond orbital that corresponds to the δ* orbital formed by negative overlapping, $d_z^{2(1)} - d_z^{2(2)}$ In addition, $d_{xz}^{(1)} + d_{xz}^{(2)}$ and $d_{yz}^{(1)} + d_{yz}^{(2)}$ participates in the π bond formation; both bonds are equivalent yet orthogonal, forming a degenerating pair. Relative to the δ* orbitals, the negative overlap of orbitals in π bonding results in corresponding π* orbitals. The combination of the d_{xy} orbitals, the pair dx^2- dy^2 yields δ bonds and δ* anti-bonds. The involvement of the dx^2- dy^2 orbitals are of utmost importance in metal-ligand binding in dirhodium complexes for example, acetate ligands overlaps with the dx^2- dy^2 orbital to form the metal-ligand bridge.[24] The δ bond results when a filled orbital of a δ-type of a ligand ($C \equiv N$) donates or transfers electron density into an empty δ* orbital of the dirhodium complexes. The cyano-coordinated bond length is possibly the longest known.

X-ray crystallographic studies performed during the synthesis and characterization of 2,2-cis-[Rh_2(NPhCOCH3)$_4$] complexes have made important revelations[24] such as:

- Rh-Rh-N bond angles for complexes of two equivalents were same;
- Rh-N-C bond angle were bent and exhibited some similarities and some other differences for different complexes.
- The average bond length of Rh-Rh was measured as 2.42 Å.

The torsion angles were also determined to predict how available the catalytic site is as they represent the elevation of the twisted molecule from planarity. It was inferred that too high torsion angles reduce the binding efficiency of the catalytic site on the rhodium atom. Figure 2 is the molecular diagrams of the twelve isomers of the $Rh_2(NPhCOCH_3)_4$ tolunitrile complexes

depicting their structures.

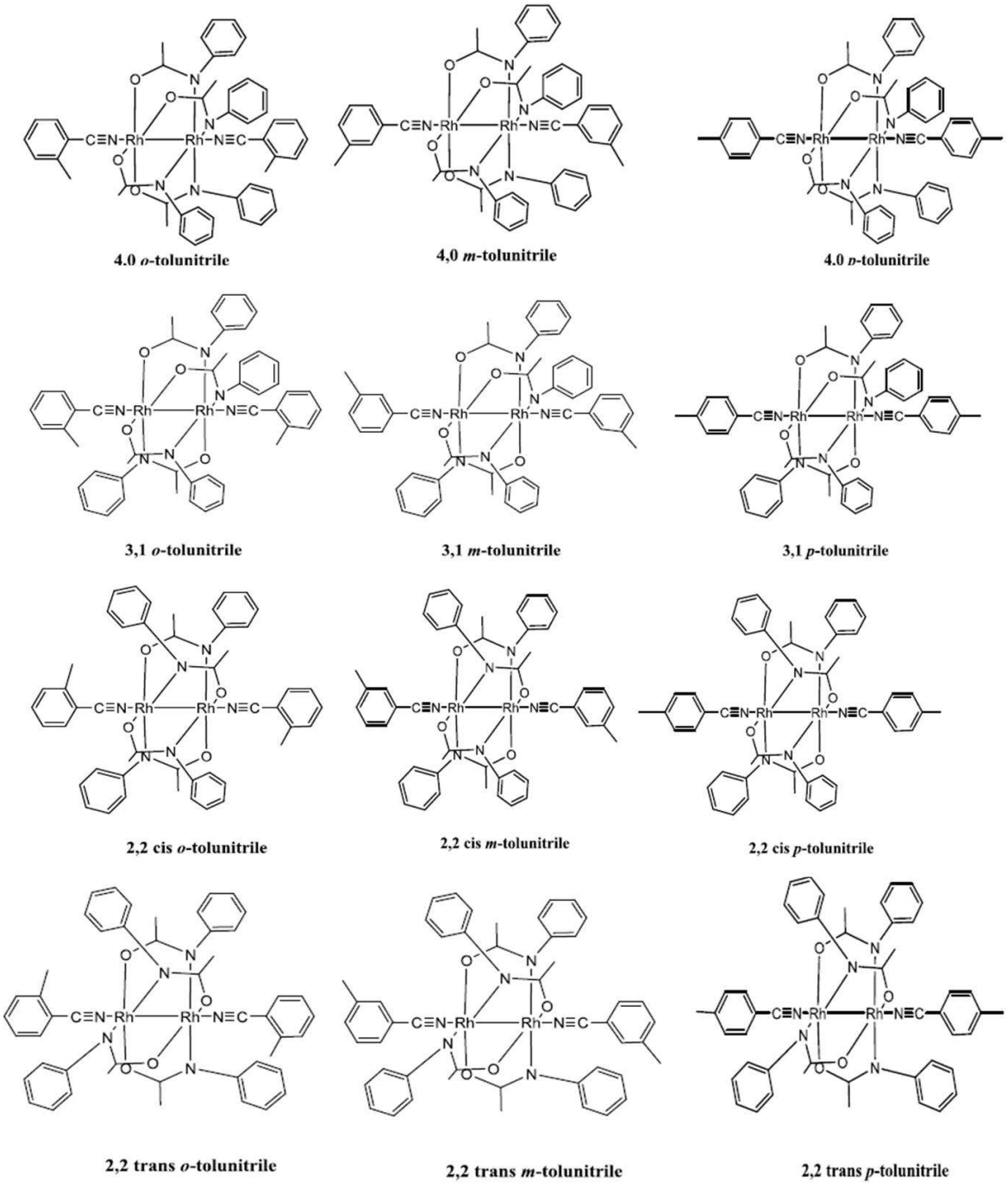

Figure 2: ChemDraw® representations of the isomeric structures of the $Rh_2(NPhCOCH_3)_4(CH_3C_6H_9CH_3)_2$

Catalysis

In a dirhodium catalyst, the complex attaches to a carbene at its catalytic site. The binding takes place during cyclopropanation reaction and the reaction involves the formation of a carbenoid as an intermediate species. Structurally, the carbenoid is formed of a metal atom bound to the neutral divalent carbine (an electrophile). The reactivity of carbenoids is dependent on the structural changes conferred to the bridging ligands of the catalyst, resulting in improvised selective catalyst. The short lives of the carbenes make it difficult to isolate and characterize the rhodium carbenoid directly.[25,26]

The four possible isomers of the amide-based dirhodium complexes (2,2-cis, 2,2-trans, 3,1-, 4,0-) will coordinate to a nitrile-containing ligand at one of the available axial sites of the rhodium atoms. The usual explanation for the coordination of the nitrile is donation of the nonbonding electrons on the nitrogen into the empty d_x^2 orbital on the rhodium to form a "σ bond" (see Figure 3). The linear Rh-N-C angle is further rationalized by donation of electrons from the perpendicular rhodium d orbital into the empty π* on the nitrile to create a "π-back bond" (see Figures 3 and 5). The orbitals involve in nitrile π-back bond with rhodium are similar to those creating π-back bond between carbene and rhodium atom.[27] (see Figures 4 and 5). This trend explains both the bonding and the usually observed geometries for the known $Rh_2(CO_2R)_4NCR$ structures. However, this explanation is insufficient for the carboxylamidate complexes.

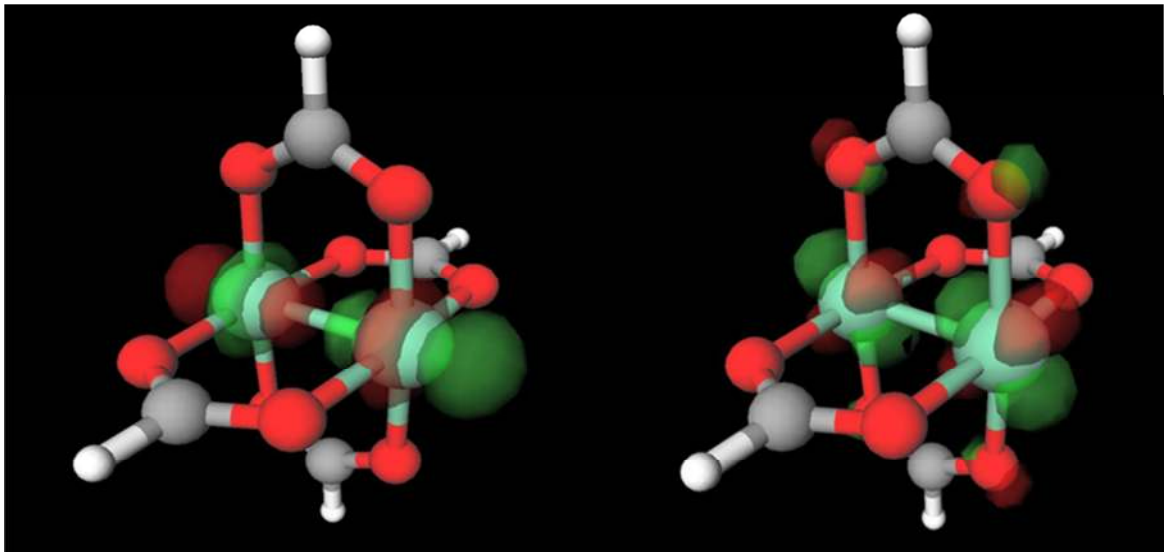

Figure 3: Molecular orbital pictures for the LUMO and HOMO-1 for $Rh_2(CO_2H)$.

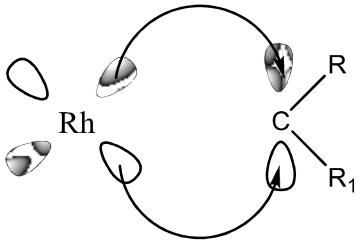

Figure 4: A π-back forming between Rhodium metal and carbene .[27]

Figure 5: The rhodium-carbene bond orbitals and rhodium–nitrile bond orbitals creating π-back bonding.[27]

Research Aims

The goals for this research were:

1- To use both *ab initio* and semi-empirical calculations for a series of dirhodium complexes in order to improve understanding of the nature of chemical bonding in this class of homogeneous catalysts.

2- To calculate the energy for the four possible isomers of the amide-based dirhodium complexes and to interpret the experimental data obtained by Dr. Eagle's research group which showed that there are significant differences in the isomeric ratio of the products of synthesis of these carboxylamidate complexes.

3- To show that the structure and bonding in dirhodium complexes is influenced by a bonded ligand using (NC^-, NCH, $NCCH_3$, and NCC_6H_5) as axial ligands.

CHAPTER 2

QUANTUM MECHANICS

The evolution of the quantum mechanics dates back towards the end of the 19th century, when the physical world was studied experimentally, and explained according to classical mechanical principles. Quantum mechanics is a contradiction to the classical mechanics. To bridge the gap where the classical mechanical principles proved flawed, it studies the matter's or the particle's nature at a microscopic level-atoms and molecules and sub-atomic entities.[28]

In 1690, Christiaan Huygens postulated the wave nature of the light. Approximately in 1704, Sir Isaac Newton postulated that light is composed of tiny particles. Although both the theories were experimentally supported, neither the complete particle theory nor the complete wave theory could explain the dual behavior of the particle under study. Most importantly, works of Louis De Broglie and that of Davisson and Germer, substantially proved that every quantum particle has a characteristic wave function. Their findings assert that matter exists as a particle in addition to wavelike behavior. Werner Heisenberg postulated that an intrinsic uncertainty is associated with the dual nature of the particle-wave, whenever the system of interest is measured.[28] Therefore, for example, the position and the momentum of a particle cannot be determined simultaneously, that is, if any one variable, particle position or momentum, is measured accurately, then the determined value of the other is less accurate.[28]

The Schrödinger Equation

The particle state in quantum physics is described in terms of time and a wave function. A wave function represents the coordinate function of the particle in question, guarding the action of the operating physically-measurable-quantity upon the particle. Therefore, the operators

of quantum mechanics have eigenvalues corresponding to each physically-measurable-quantity, and one dependent on a wave function. The mathematical representation of this correlation was first developed by an Austrian physicist, Erwin Schrödinger in 1926. This differential equation is popularly known as the Schrödinger equation. Again, this eigenvalue equation governs the change in the evolving wave functions with respect to time. Thus, the time-dependent Schrödinger equation[29-31] for a single particle moving in the three dimensions, is

$$i\hbar\frac{\partial\Psi(r,t)}{\partial t} = -\frac{\hbar^2}{2m}\nabla^2\Psi(r,t) + V(r)\Psi(r,t) \qquad (2\text{-}1)$$

where $\hbar$ is the reduced Planck's constant and equals to $h/2\pi$, h is Planck's constant and V(r) is the potential energy of the field in which the particle of mass (m) is moving, $\Psi(r,t)$ is the wave function and ∇^2 represents the second order differential Laplacian operator.

This time dependent equation does not account for spin and/or relativistic effects. Moreover, as the potential energy in the equation is time independent, the total energy of the system is conserved. A time-independent equation results if the wave function, as the spatial and temporal product (*i.e* $\Psi(r,t) = \Psi(r)f(t)$), is written into the Equation 2-1:[32]

$$\Psi(r)i\hbar\frac{df(t)}{dt} = f(t)\left[-\frac{\hbar^2}{2m}\nabla^2 + V(r)\right]\Psi(r) \qquad (2\text{-}2)$$

or,

$$\frac{i\hbar}{f(t)}\frac{df}{dt} = \frac{1}{\Psi(r)}\left[-\frac{\hbar^2}{2m}\nabla^2 + V(r)\right]\Psi(r) \qquad (2\text{-}3)$$

Since, in the above equation expression on the left side is a time-function while the right side is a position-function, both the sides must equal to a constant. Substituting E as the dimension of energy on the right-hand side of the expression, two partial derivative equations can be extracted:

$$\frac{1}{f(t)}\frac{df(t)}{dt} = -\frac{i\mathrm{E}}{\hbar} \tag{2-4}$$

and

$$-\frac{\hbar^2}{2m}\nabla^2\,\Psi(\mathrm{r}) + V(\mathrm{r})\Psi(\mathrm{r}) = \mathrm{E}\,\Psi(\mathrm{r}) \tag{2-5}$$

Equation 2-5 is a time-independent Schrödinger equation. Further solving Equation 2-4 yields $f(t) = e^{-iEt/\hbar}$. Since the Hamiltonian operator in the Equation 2-5 is Hermitian generating a real eigenvalue, E is real. For the given facts that E is real and $e^{\pm i\theta} = cos\theta \pm sin\theta$ (Euler's formula), $f(t)$ has constant magnitude and solutions to it is harmonic in time. In quantum mechanics, Hamiltonian operator is described as the total of the operators of kinetic energy and the potential energy of the system. Designating Hamiltonian operator as $\hat{\mathrm{H}}$, the Equation 2-5 can be rewritten as an eigenvalue equation:

$$\hat{\mathrm{H}}\,\Psi = \mathrm{E}\,\Psi \tag{2-6}$$

Furthermore, the kinetic energy of a system is the summation of individual kinetic energies of the particles in the system, *i.e.*

$$T = \frac{-\hbar^2}{2m}\sum_n\left[\frac{\partial^2}{\partial x^2} + \frac{\partial^2}{\partial y^2} + \frac{\partial^2}{\partial z^2}\right] \tag{2-7}$$

Similarly, the potential energy of the system is measure of combined electrostatic forces between the particles in that system.

$$\mathrm{V} = \frac{1}{4\pi\varepsilon_0}\sum_l\sum_{m<l}\frac{q_l q_m}{r_{lm}} \tag{2-8}$$

where q_l and q_m are the electrostatic charges on the $l^{th}$and m^{th} particles respectively, and ε_o is the permittivity of the free space.

The boundary conditions for the specific problem of interest states wherein the particles are restricted to a limited space, impose restrictions on the particle position. Therefore, the solution for the wave function must satisfy the condition of its normalization to unity or else, it will be a deviation from the probability interpretation of the wave function. To determine the probability intensity of the particle, Schrödinger proposed:

$$I = \psi(x)^* \psi(x) \tag{2-9}$$

where I is the probability intensity, and $\Psi(x)^*$ is the wave function's complex conjugate. Later, Born interpreted that the square of the wave function is proportional to the intensity of the particle in the region of space limited by the boundary elements.

A rotating particle has quantized angular momentum. Subatomic particles like protons, electrons, neutrons, and photons, are characterized by a "spin" that is a degree of freedom transferring angular momentum under rotation. In a uniform field, the spin-dependent Hamiltonian operator does not contain explicit coordinates. Hence the wave function of a particle is the product of spin as well as coordination function,

$$\psi(\mathrm{r})\, g(m_s) \tag{2-10}$$

where $\Psi(\mathrm{r})$ is the wave function of free motion and $g(m_s)$ denotes either α or β functions, dependent on m_s values (-½ or ½, -1 or 1,0). It is a purely quantum phenomenon with no analogy in classical physics.[33] Since the spin variable doesn't count, the Hamiltonian operator for the single of the particle is given by:

$$\hat{H}\,[\psi(\mathrm{r})\, g(m_s)] = E\,[\psi(\mathrm{r})\, g(m_s)] \tag{2-11}$$

The direct consequence of this phenomenon is that the particle energy is free of the actual spin state, *i.e.* $\psi\alpha$ and $\psi\beta$.

The detailed description of the quantum mechanics of a multi-electron species is evident after understanding the concepts of the electron indistinguishability. According to the Pauli's exclusion principle,[34] no two wave functions or spin function, of electrons must be symmetrical in the inter-exchange of any two electrons:

$$\psi (q_1, q_2,..q_n) = - \psi (q_1, q_2,..q_n) \qquad (2\text{-}12)$$

All particles with half-spin, referred to as fermions (such as electrons) obey Fermi-Dirac statistics and therefore, have anti-symmetric wavefunctions, whereas symmetric wavefunctions is the requirement of all the particles with integral spin, bosons, and these follow Bose-Einstein statistics.

Approximation Methods

The many-particle Schrödinger differential equation yields non-analytic solutions. Solving chemical problems in quantum mechanics, requires more effective methods which upon implementation yields approximate solutions to the eigenvalue equations. Ignoring the interactions such as spin-orbit coupling and relativistic effects, and taking into account that the nuclei and electrons are point masses, the Hamiltonian operator of the molecule is given by:[29]

$$\hat{H} = T^{elec} (r) + T^{nuc} (R) + V^{nuc\text{-}elec} (R, r) + V^{elec} (r) + V^{nucl} (R) \qquad (2\text{-}13)$$

where R and r denotes the degrees of freedoms of the nuclei and the electrons respectively.

One of the remarkable consequences of the application of the Schrödinger equation to the motions of nuclei and electrons in a molecule is the chemist's perception of the microscopic electronic energy surfaces on which interactions like transitions, rotations and vibrations takes

place.[35] Solutions of the Born-Oppenheimer approximation to the Schrödinger equation governing the inter-particle motions and potential energies of the electrons and nuclei of an atom/molecule/ion, actually solves two distinct problems.[35] In the first problem, it solves the electronic Schrödinger equation for the nuclear geometry-dependent wave functions and energies of the electrons. In the second problem, the method solves for the Schrödinger equation to give an exact solution to the vibration/rotation for the nuclei moving on a particular electronic energy surface. Thus, with the dissolution of degrees of freedoms of the electrons and nuclei in a species, the exact Hamiltonian equation purely for the motion of electrons is given by:

$$\hat{H} = -\frac{\hbar}{2m_\alpha}\sum \nabla_i^2 - \sum_\alpha \sum_i \frac{Z_\alpha e^2}{r_{i\alpha}} + \sum_j \sum_{i>j} \frac{e^2}{r_{ij}} \qquad (2\text{-}14)$$

where i and j are the i^{th} and j^{th} electrons, respectively and α represents the α^{th} nuclei, $r_{i\alpha}$ is the distance between the i^{th} electron and the α^{th} nucleus, z_α is the charge on the α^{th} nuclei and is the distance between the i^{th} and j^{th} electron.

The nuclear repulsion is of substantial order and cannot be ignored in this case. The term nuclear repulsion, V_{NN}, is given by:

$$V_{NN} = \sum_\alpha \sum_{\beta > \alpha} \frac{Z_\alpha Z_\beta e^2}{r_{\alpha\beta}} \qquad (2\text{-}15)$$

and the electronic Hamiltonian is $\hat{H}_{el} + V_{NN}$ (2-16)

Considering Equation 2-14, the right-hand side consists of three terms. The first term is the operator for the electronic kinetic energy, the second term represents the coulombic electron-nuclei attraction, and the third term represents the coulombic electron-electron repulsions. The Born Oppenheimer approximation method does not account for the relativistic effects.

There are several approximation methods, including the Born Oppenheimer approximation method as discussed above. Two other approximation methods: the Hartree–Fock Self Consistent Field Theory (HF-SCF), and DFT are further discussed in this study.

Hartree–Fock Self Consistent Field Method

The rationale behind the development of the Hartee-Fock theory was to extract the exact solution to the electronic Schrödinger equation that derived from the application of the Born Oppenheimer approximation method to the time-independent Schrödinger equation.[36]

Indeed, determination of the exact wave function for the hydrogen atom is possible but this is not the case with other atoms having higher atomic weight. For small systems like helium or lithium, by incorporating the inter-electronic distances as functions in solving the variational equation, it is feasible to calculate the exact wave functions. The Hamiltonian operator for the two electrons in the n-electrons system is given by:

$$\hat{H} = -\frac{\hbar}{2m_e}\sum_{i=1}^{n}\nabla_i^2 - \sum_{i=1}^{n}\frac{Z_\alpha e^2}{r_{i\alpha}} + \sum_{i=1}^{n-1}\sum_{j=i+1}^{n}\frac{e^2}{r_{ij}} \qquad (2\text{-}17)$$

where the first term is the value of the n-electronic kinetic energy and electron-ion potential in total, the second term is the total of the electrostatic potential energy of the nucleus-electron interactions (charge on the nuclei Ze, Z = n for neutral atoms), and the last term represents the inter-electronic repulsion; the j=i+1 is a restrictive term that avoids repeating inter-electronic repulsion, and avoid terms like e^2/r_{ij}. Equation 2-7 assumes that the wave function is the operator corresponding to the single orbital occupied by the electrons. The first two terms are the single operator sum, each act on a single electronic coordinate, whereas the last term is a pair of operators that act on electron pairs. Since the probability of the like-spin in the vicinity of an

electron surrounded by an "exchange hole", than the mean field represented by the last term of Equation 2-17 would imply.[37] Thus, for $i = j$, the inter-electronic interaction cancels out. Expressing the zeroth-order wave function as he product of n electronic orbitals in hydrogen-like species (one-electron system), as:

$$\Psi^{(0)} = f_1(r_1, \theta_1 \emptyset_1)\ f_2(r_2, \theta_2, \emptyset_2), \ldots \ldots f_n(r_n, \theta_n, \emptyset_n) \tag{2-18}$$

where the single-particle wave function is given by:

$$f = \mathrm{R}_{nl}(r)\ \mathrm{Y}_l^m(\theta, \emptyset) \tag{2-19}$$

$\mathrm{R}_{nl}(r)$ is the radial component of the orbital in hydrogen-like species and expressed as:

$$\mathrm{R}_{nl}(r) = \left\{\frac{(n-l-1)!}{2n\ \{(n+1)!\}}\right\}^{\frac{1}{2}} \left(\frac{2}{na_0}\right)^{l+3/2} r^l e^{-r/na_0}\ L_{n+1}^{2l+1}\left(\frac{2r}{na_0}\right) \tag{2-20}$$

where the Laguerre polynomials, $L_{n+1}^{2l+1}\left(\frac{2r}{na_0}\right)$, are associated with quantum numbers n and l. Spherical harmonics, $Y_l^m(\theta, \varphi)$, are expressed as:

$$\left[\frac{(2l+1)(l-|m|)!}{4\pi\ (l+|m|)!}\right]^{1/2} P_l^{|m|}\cos(\theta)\ e^{im\emptyset} \tag{2-21}$$

Here, the associated Legendre polynomials are $P_l^{|m|}\cos(\theta)$.

The approximate solution to the wave function in Equation 2-18 given by the Hartree-Fock method, fails to satisfy the antisymmetric principle. A variational method is, therefore, adapted to overcome this limitation. Equation 2-18 can be rewritten as:

$$\Phi = g_1(r_1, \theta_1 \emptyset_1)\ g_2(r_2, \theta_2, \emptyset_2), \ldots \ldots g_n(r_n, \theta_n, \emptyset_n) \tag{2-22}$$

If the variational integral is minimized by the g_i functions in atomic calculations, then the ground energy of the state of the system, E_1, is given by:

$$\mathrm{E}_1 \leq \frac{\int \emptyset^* \hat{\mathrm{H}} \emptyset\, d\tau}{\int \emptyset^* \emptyset\, d\tau} \tag{2-23}$$

where,

$$g_i = h_i\,(r_i)\; Y_{li}^{m}\,(\theta_i, \emptyset_i) \tag{2-24}$$

Hartree's Procedure

An iterative method was introduced by D. R. Hartee in 1928 for calculating the g_i. The approximation method is called a the Hartree Self-Consistent Field method (HF-SCF method).[37]

The HF-SCF method finds its application in calculating wave functions of the multi-electronic systems. The self-consistent field is the set of orbitals, a solution to the Hartee-Fock equation, *i.e* change in V_{ion}.

The strategy is to construct a Hamiltonian by guessing some wave functions, in solving the Schrödinger equation. Denoting s_1 to the product of the normalized function of r and a spherical harmonic the product wave function is:

$$\phi = s_1\,(r_1, \theta_1\, \emptyset_1)\; s_2\,(r_2, \theta_2, \emptyset_2)\ldots\; \ldots s_n\,(r_n, \theta_n, \emptyset_n) \tag{2-25}$$

The mean field approximation is made, that is the inter-electronic electrostatic interactions are averaged. Considering that there is an on-going interaction between electron (q_1) -electron (q_2) and each are associated with a continuous charge distribution, Coulomb's law solves for the potential energy,

$$V_{12} = \frac{1}{4\pi\varepsilon_0}\frac{q_1 q_2}{r_{12}} \tag{2-26}$$

The charge distribution is determined by charge density, ρ_2, which is charge per unit volume. If the average interactions between q_1 and the infinitesimal q_2, and the r_{12} is the distance

of the first electron (q_1) from the charge distribution with the density measure ρ_2, the infinitesimal charge $\rho_2 dv_2$ in an infinitesimal volume dv_2 is

$$V_{12} = \frac{q_1}{4\pi\varepsilon_0} \int \frac{\rho_2}{r_{12}} dv_2 \tag{2-27}$$

Denoting the probability density $|s_i|^2$ of the electron *i,*

$$\rho_2 = -e|S_2|^2 \tag{2-28}$$

Therefore, for the second electron, the probable density is:

$$V_{12} = \frac{e^2}{4\pi\varepsilon_0} \int \frac{|S_2|^2}{r_{12}} dv_2 \tag{2-29}$$

Adding all the n-electronic interactions, extracting from the Equation 2-29,

$$V_{12} + V_{13} + \ldots\ldots + V_{1n} = \sum_{j=2}^{n} \frac{e^2}{4\pi\varepsilon_0} \int \frac{|S_j|^2}{r_{1j}} dv_j \tag{2-30}$$

and the nucleus-electron 1 ionic potential energy is

$$V(r_1, \theta_1, \emptyset_1) = \sum_{j=2}^{n} \frac{e^2}{4\pi\varepsilon_0} \int \frac{|S_j|^2}{r_{1j}} dv_j - \frac{Ze^2}{4\pi\varepsilon_0 r_1} \tag{2-31}$$

In the central field approximation, the function of *r* corresponds to the effective potential operator that acts upon an electron. So, when the $V_1(r_1, \theta_1, \emptyset_1)$ is averaged over the θ angle and the φ angle, Equation 2-31 gives

$$V_1(r_1) = \frac{\int_0^{2\pi}\int_0^{\pi} V(r_1,\theta_1,\emptyset_1) \sin\theta_1 \, d\theta_1 d\emptyset_1}{\int_0^{2\pi}\int_0^{\pi} \sin\theta_1 \, d\theta_1 d\emptyset_1} \tag{2-32}$$

Rewriting the one-electron Schrödinger equation as

$$\left[-\frac{\hbar^2}{2m_e} \nabla_1^2 + V_1(r_1)\right] t_1(1) = \varepsilon_1 t(1) \tag{2-33}$$

The approximate solution to the Schrödinger equation by HF-SCF methods, determines the evolving wave functions t_1 and ε_1. In this calculation, a set of orbitals, commonly called the Hartree-Fock orbitals, is obtained iteratively, and the output wave function is compared with the input wave function. The compared set of wave functions is further tested to satisfy the required

numerical convergence criterion. The convergence fails if the tested wave functions varied, and the iteration is repeated until both wave functions are the same or self-consistent. The following differential equation is used to determine the set of orbitals or the Hartree-Fock orbitals:

$$\widehat{F}\, t_i(i) = \varepsilon_i\, t_i(i) \tag{2-34}$$

From the Equations 2-33 and 2-34, the Hartee-Frock $\widehat{F}$ is:

$$\widehat{F}\, t_i(i) = \left[-\frac{\hbar^2}{2m_e}\, \nabla_1^2 + V_1(r_1)\right] \tag{2-35}$$

The SCF approximation method seeks orbital energy solutions to the one-electron Schrödinger equation. A correcting factor is introduced to refrain the iteration process of counting the electronic- repulsion terms again and again. The correcting term is given as

$$E = \sum_{i=1}^{n} \varepsilon_i \; - \sum_{i=1}^{n-1} \sum_{j=i+1}^{n} \iint \frac{e'^2 |g_i(i)|^2 |g_j(j)|^2}{r_{ij}} dv_i dv_j \tag{2-36}$$

The first summation term denotes the total orbital energies, whereas the second double-summation term accounts for the twice counting the potential-energies sum. Therefore, denoting the energy associated with the i_{th} spin-orbital as ε_i and that of the spin orbital as μ_i the resultant expression is:

$$\widehat{F}\, \mu_i = \; \varepsilon_i\, \mu_i \quad i = 1, 2, 3\ldots, \text{n} \tag{2-37}$$

The SCF orbital problems requires considering the variations of the spin-orbitals of the single-electron species that are largely determined by two main constraints: the normalization of the spin-orbitals, and the orthogonality.

The variation principle inspires the Hartree-Frock strategy to obtain SCF solutions to the n-electron Schrödinger equation. Therefore, a spin-orbital results whenever a spatial orbital φ_i is multiplied to the either of spin functions, α or β. The spin-orbital Slater determinants represents the Hartree-Fock wave function of the molecule.

$$\Psi = \frac{1}{\sqrt{N!}} \begin{vmatrix} \emptyset_1(1)\,\alpha_1 & \emptyset_1(1)\,\beta_1 & - & - & \emptyset_N(1)\,\alpha_1 & \emptyset_N(1)\,\beta_1 \\ \emptyset_1(1)\,\alpha_2 & \emptyset_1(1)\,\beta_2 & - & - & \emptyset_N(1)\,\alpha_2 & \emptyset_N(1)\,\beta_2 \\ - & - & - & - & - & - \\ - & - & - & - & - & - \\ \emptyset_1(1)\,\alpha_N & \emptyset_1(1)\,\beta_N & - & - & \emptyset_N(1)\,\alpha_N & \emptyset_N(1)\,\beta_N \end{vmatrix} \quad (2\text{-}38)$$

Assuming that the Hamiltonian term for the nuclear repulsion is $\widehat{H}_{el}$, and V_{NN} as the ionic potential energy, employing the variation principle to extract SCF solutions, the Hartree-Fock equation for the molecular electronic energy, E_{HF} is:

$$E_{HF} = \langle \Psi \left| \widehat{H}_{el} + V_{NN} \right| \Psi \rangle \quad (2\text{-}39)$$

where Ψ is the Slater determinant Hartree-Fock wave function. The HF energy for a polyatomic or a closed shell diatomic molecule is given as[38]

$$E_{HF} = 2 \sum_{i=1}^{n/2} H_{ii}^{core} + \sum_{i=1}^{n/2} \sum_{i=1}^{n/2} (2\,J_{ij} + K_{ij}) + V_{NN} \quad (2\text{-}40)$$

where J_{ij} is the coulomb integral, K_{ij} is the exchange integral and H_{ii}^{core} is the one electron core Hamiltonian. The $\emptyset_i$ orbital minimizes the variational integral, E_{HF}. Since the orthogonality of the orbitals is assumed to be a bounding condition, $\emptyset_i$ must satisfy the following differential equation:

$$\widehat{F}\,(1)\,\emptyset_i\,(1) = \varepsilon_i\,\emptyset_i\,(1) \quad (2\text{-}41)$$

As $\emptyset_i$ is normalized, the integration- solution of the product of the φ_i and the Equation 2-41, is the orbital energy-expression:

$$\varepsilon_i = \int \emptyset(1) \widehat{F}\,(1)\,\emptyset_i\,(1)\,dv_i \quad (2\text{-}42)$$

or,

$$\varepsilon_i = H_i^{core} + \sum_{j=1}^{n/2} (2\,J_{ij} - K_{ij}) \quad (2\text{-}43)$$

Substituting the solution of the $\sum_{i=1}^{n/2} H_{ii}^{core}$ into Equation 2-40, yields an HF energy solution.

$$E_{HF} = 2 \sum_{i=1}^{n/2} \varepsilon_i + \sum_{i=1}^{n/2} \sum_{i=1}^{n/2} (2 J_{ij} + K_{ij}) + V_{NN} \tag{2-44}$$

A more accurate method to calculate molecular SCF orbitals employs the finite expansion of the spatial orbitals as a linear combination of the atomic orbitals, X_s, as proposed by Roothan.

$$\emptyset = \sum_{s=1}^{b} C_{si} X_s \tag{2-45}$$

From the Equations 2-44 and 2-45,

$$\sum_{s=1}^{b} C_{si} \hat{F} X_s = \varepsilon_i \sum_{s=1}^{b} C_{si} X_s \tag{2-46}$$

Multiplying X_r to the above equation, and then, integrating,

$$\sum_{s=1}^{b} C_{si} (\hat{F}_{rs} - \varepsilon_i S_{rs}) = 0 \quad ; r = 1,2,,,,,,b \tag{2-47}$$

For non-identity solutions, the secular determinant coefficients cancel out. Hence,

$$det\ (\hat{F}_{rs} - \varepsilon_i S_{rs}) = 0 \tag{2-48}$$

The variable C_{si} is determined by solving the HF-Roothan equation[39] iteratively. The downside of the HF-SCF theory is that it neglects the correlation between the electron-motions. Since the Pauli's exchange interactions (correlation interactions) are not accounted among the electrons, therefore, the term for the correlation energy is missing in HF procedure. All those *ab initio* methods that go beyond the Hartree-Fock approximation are structured in a way to recover maximum correlation energy within the permissible limits of their basis sets. The correlation

energy measures the variation in the exact energy, E_{exact}, and the calculated energy (by HF-SCF method), E_{HF}, of the system:

$$E_c^{HF} = E_{exact} - E_{HF} \quad (2\text{-}49)$$

Experiments as well as the computing methods like coupled cluster calculations [40-42] can be used to determine the exact energy.

Density Functional Theory

DFT has long been the mainstay of ground-state electronic calculations in computational sciences, and condensed-matterphysics.[43] It is not just another traditional *ab initio* method or way of parameterizing empirical solutions and it is applied to much larger systems as it maps any interacting problem exactly to a much simple dimensional problem.[43] Computing by the DFT method requires determination of a molecule's electron density to derive the molecular properties. The electron density represents one of the overall spatial variables and is defined as the integral over the spin coordinates of all the electrons. Thus, DFT makes use of physical characteristics of all molecules as an electron density rather than a mathematical construct, a wavefunction, with no physical reality. It is to be noted that the electron energy (E), here, is a function of electron density (ρ). If $\rho_{(r)}$ is the overall electron density of the molecule at a particular point in space r, then the electronic energy, $E(\rho)$, is a functional, that is function of a function.

In 1927, L. H. Thomas and E. Fermi independently formulated the first Density Functional Theory, also known as the Statistical Theory, to describe the electron density, $\rho(r)$, and the ground state energy, $E_{(n)}$, for large n-electronic atom or molecule system.[44] According to Thomas, "electrons are distributed uniformly in the six dimensional phase space for the motion

of an electron at the rate of two for each h^3 of volume" and the resulting effective potential field "is itself determined by the nuclear charge and this distribution of electrons." [45] Dirac extended this assumption to the time dependent domain in order to describe the excited states. Thus, using the uniform electron gas model, Thomas, Fermi and Dirac gave the first density functional. Although the kinetic energy, E^T, of the electron-system has been approximated as an explicit density functional, but the theory is a miss on accounting the inter-electronic exchange, E^J, and correlation, E^{XC}, between the motions of the electrons. Instead, Dirac employed a local approximation for exchange yielding the electronic energy functional in an external potential, E^V.

$$E_{TF}[\rho] = E^T[\rho] + E^V[\rho] + E^{XC}[\rho] \tag{2-50}$$

The resultant exchange energies, E^J, are roughly 10% smaller than the same from HF theory. Moreover, the spurious electronic self-interaction does not exactly cancelled. Dirac's assumption was based on uniform electron densities, which is not the actual case. Therefore, there is a need for an improvised functional for the systems with inhomogeneous densities. The correction came through Kohn and Sham method in 1965, wherein the calculations exactly accounted for the majority of the kinetic energies.[46] A good exchange correlation energy functional is expressed as the total of the exchange and correlation functional involved in the molecular interaction-calculations. The kinetic energy of the independent particle, when separated from the long-range terms in HF calculations, results an exact approximation of the exchange-correlation energy, E^{XC} as a nearly local or local density functional.[47]

$$E^{XC} = \int dr\rho(r)\varepsilon^{xc}([\rho], r) \tag{2-51}$$

where ε^{xc} is the ρ-dependent energy per electron functional in a point r.

The exchange-correlation energy functional ($E_{xc}(\rho)$) in the local-density approximation (LDA) depends solely on the density at the coordinate where the functional is evaluated. So,

$$E_{xc}^{LDA}(\rho) = \int \varepsilon_{xc}(\rho)\,\rho(r)\,dr \tag{2-52}$$

The $E_{xc}(\rho)$ is further dissolved into the exchange, E_x, and correlation, E_c, terms linearly:

$$E_{xc}(\rho) = E_x + E_c \tag{2-53}$$

so that individual expression for solving the E_x and E_C terms, are sought. The functional corresponding to the uniform electron gas is used for the E_x. Several different approximations are determined for E_c, by the limiting expressions for the correlation density. Expression for the approximation of the exact exchange energy of a homogenous free electron gas in the terms of Dirac exchange energy and LDA exchange energy:[48]

$$E_{xc}^{LDA}[\rho] = \frac{3}{2}\alpha K_D[\rho] = -\frac{9}{8}\alpha \left(\frac{3}{\pi}\right)^{\frac{1}{3}} P^{\frac{4}{3}}(r)\,dr \tag{2-54}$$

It is to be worth noticing that the LDA exchange energy accounts only 10% of the error in the HF exchange energy.[49] The Dirac exchange energy formula is denoted as $K_D[\rho]$ whereas α is an empirical constant for the system under study and has a value of 2/3 when calculated for a uniform free electron gas.

The Kohn-Sham Local Density Approximation (KS-LDA) fell short in the calculations involved in non-homogeneous systems and therefore, Kohn-Sham Local-Spin Density Approximation (KS-LSDA) serves as a correction. Where the LDA for exchange energy functional is:

$$E_{xc}^{LDA}[\rho^{\alpha}, \rho^{\beta}] = 2^{\frac{1}{2}} C_X \int ((\rho^{\alpha})^{\frac{4}{3}} + (\rho^{\beta})^{\frac{4}{3}})\,dr \tag{2-55}$$

where β measures the difference between the total spin density and the α spin density. The expression for the spin polarization energy is:

$$\varsigma = \frac{\rho^{\alpha} - \rho^{\beta}}{\rho} = \frac{\rho^{\alpha} - \rho^{\beta}}{\rho^{\alpha} + \rho^{\beta}} \tag{2-56}$$

From the Equations 2-55 and 2-56, the spin polarization-dependent exchange energy expression can be written as

$$E_{LSD}^{X} = \int \rho\, \varepsilon^{x}(\rho, \varsigma)\, dr \tag{2-57}$$

where

$$\varepsilon^{x}(\rho, \varsigma) = \varepsilon_{x}^{0}(\rho) + [\varepsilon_{x}^{1}(\rho) - \varepsilon_{x}^{0}(\rho)]\, f(\varsigma) \tag{2-58}$$

To observe the dependence on the spin polarization, the exchange energy density can be realized as an interpolation between the limiting values of "paramagnetic" ($\varsigma = 0$) and "ferromagnetic" ($\varsigma = 1$) cases.[37] Spin density, ρ, is zero for the closed shell and is one for the open-shell systems. Again, if the system is unpolarized systems (closed shell, B3LYP), ρ is zero and is in between zero and one for the polarized systems (open-shell system, UB3LYP). If the product of the total spin density ρ and $(\varsigma + 1)$ is halved, the result is the spin.

LDA is the easiest possible density functional approximation, and as discussed earlier in this section, it improvises HF. More sophisticated General Gradient Approximations (and hybrids) reduce the typical error by about a factor of 5 (or more) in LDA, by imposing the exact exchange hole on the approximate hole.[43]

$$E_{GGA}^{X} = -\frac{3}{4}\left(\frac{3}{\pi}\right)^{\frac{1}{3}} \int dr \rho^{\frac{4}{3}}(s) \tag{2-59}$$

with

$$S = \frac{|\nabla \rho\,(r)|}{2K_F \rho} \tag{2-60}$$

$$K_F = (3\pi^2 \rho)^{\frac{1}{3}} \tag{2-61}$$

and

$$F(s) = (1 + 1.296S^2 + 14S^4 + 0.2S^6)^{\frac{1}{15}} \tag{2-62}$$

Expression of the hybrid functional B3LYP

$$E_{B3LYP}^{XC} = (1- a)\, E_{LSDA}^{X} + aE_{HF}^{X} + bE_{B88}^{X} + (1 - c)E_{LSDA}^{C} + cE_{LYP}^{C} \qquad (2\text{-}63)$$

B88 is the Becke's exchange functional and LYP represents Lee-Young-Parr correlation functional. The above equation contains the HF terms and the DFT terms.

According to the Kohn-Sham Theory,

$$F\,(1) = -\tfrac{1}{2}\,\nabla_1^2 \; - \; \sum_{\alpha} \frac{Z_\alpha}{r_{1\alpha}} + \; \sum_j J_j\,(1) + V^{XC} \qquad (2\text{-}64)$$

$$V^{XC} = \frac{\partial E^{XC}}{\partial \rho} \qquad (2\text{-}65)$$

then the Kohn- Sham orbitals, ψ_i, is given by

$$F(1)\psi = \varepsilon\psi \qquad (2\text{-}66)$$

As electron density is the total of the occupied Kohn-Sham orbitals (ψ_i):

$$\rho = \sum_i \left|\psi_i\right|^2 \qquad (2\text{-}67)$$

The hybrid functional B3LYP (Becke's three-parameter functional with the Lee-Young-Parr correlation) is the most used DFT method in chemical calculations, mostly the problems related to organic molecules.[50] Other such examples of hybrid functionals are Becke exchange, Perdew and Wang correlation (B3PW91), and Becke exchange, Perdew correlation (B3P86). DFT finds its wide application in large areas of chemistry including quantum mechanics as well as in statistical mechanics. It is a necessary tool for determination of the chemical attributes such as reactivity, electronegativity, and many more.[51]

Basis Sets

In general, a basis set is a group of coordinates defining a space wherein a calculation is to be done. Constructs like Linear Combination of Atomic Orbitals - Molecular Orbitals (LCAO-MO) make use a set non-orthogonal single-particle functions, referred as the "basis set." As per the LCAO-MO approximation, atomic orbitals combine to form molecular orbitals. Thus, an orbital represents one-electron function. The self-consistent field (SCF) wave functions of a molecule result when the spatial orbitals are expanded as a linear combination of one-electron basis functions,

$$\varphi_i = a_0 + \sum_{s=1}^{b} c_{si}\chi_s \tag{2-68}$$

where b is the numerical value of the atomic orbitals participating in the molecular orbital construct. The Slater class atomic orbital (STO) is one of the older basis set examples in computational chemistry,

$$S_{nlm}(r, \theta, \emptyset) = \frac{(2\xi)^{n+1/2}}{[(2n)!]^{1/2}} r^{n-1} e^{-\xi r} Y_l^m(\theta, \emptyset) \tag{2-69}$$

where ζ (zeta) represents the orbital exponent which controls the orbital width, that's why a large ζ gives a tight function and a small ζ gives a diffuse function. Therefore, each χ_s is a Slater Type Orbital (STO) basis functions. STO basis functions do not find much application in present-day calculations as these involve time-consuming enormous tasking in computing the secular determinants. The STO basis sets pose difficulty in solving the problems of evaluating integrals that involve multi- nuclear center. The difficulty ceased after the Gaussian-type functions (GTFs) were introduced by Boys in 1950.[52] Gaussian-type functions are almost universally used in quantum chemistry. Gaussian-type orbitals can be expressed as

$$G_{nlm}(r, \theta, \emptyset) = N_n r^{n-1} e^{-\alpha r^2} Y_l^m(\Theta, \Phi) \quad (2\text{-}70)$$

Since a basis set is a function of atomic orbital, therefore each atomic orbital can be identified from the other according to the types of basis sets used. These basis set types may be minimal (*i.e* one basis function for each orbital in an atom) used in describing the electrons of the inner-shell; double-zeta (two basis functions for each atomic orbital) for expressing the valence electrons; triple-zeta (three basis sets for each atomic orbital); and so on. The varying size functions allow expansion or contraction of an orbital in the vicinity of the approaching atom(s).

A split-valence basis uses a single Slater-orbital for each core atomic orbital, and a sum of Slater-orbitals for the valence atomic orbitals. The present study employs Pople's split-valence double-zeta basis set called 6-31G basis set on the carbon atoms, wherein total of 6 Gaussian functions used for the inner shell; the hyphen imply that a Slater-orbitals pair had been used for each 2s and 2p atomic orbitals; the digit 3 suggests that the total of three Gaussian functions represents the smallest Slater valence orbital whereas the number 1 infers that the larger valence orbital is given by a single Gaussian function. 6-31G with added d function polarization of non-hydrogen atoms are represented as 6-31G* [or 6-31G(d)] or, 6-31G** is 6-31G(d, p) implies that 6-31G* plus p function polarization for hydrogen. Similarly, 6-311G is a split-valence triple-zeta basis and it has one GTO added to 6-31G. 6-31+G is the 6-31G plus diffuse s and p functions for non-hydrogen atoms. Basis sets and diffuse functions together construct an augmented basis sets. According to the review by Papajak *et al*., an augmented basis sets is not necessary for hydrogen atoms.[53] For a carbon atom, split-valence double zeta basis sets has nine functions for the 3s2p orbitals.

As the other atoms approach, the orbitals of the considered atom may shift to one side or the other. The phenomenon is called as polarization. For example, pairing of a s-orbital with a p-

orbital can polarize the s-orbital in one direction. Similarly, p-orbitals, when mixed with the d-orbitals, polarize. So, the mixing of two basis functions with different angular momentums, say l and $l+1$, cause the polarization of the basis function with angular momentum, l. This gives polarized double-zeta, or double-zeta plus polarization basis sets, etc.

The greater the number of core electrons is, the more complex is, the calculations of the electronic wave functions in systems with higher atomic number such as the heavier elements. Thus, employing a pseudopotential is an attempt of incorporating effective core potential to replace the complicated combined effects of core electronic motions and nucleus of an atom. The use of pseudopotential construct is that it is a cost-effective computing method. This concept assumes that the core electrons are frozen and these electrons add to the nuclei to form a non-flexible and non-polarizable ion cores. Once the core states are invariant, the method solve the aforementioned problem, dealing explicitly with the valence electrons.[54]

A density expression that contains independent terms of the core and valence orbitals is:

$$n(\mathrm{r}) = \sum_{i}^{occ} \psi_i^*(\mathrm{r})\ \psi_i(\mathrm{r})$$

$$= \sum_{i \in core}^{N_{core}} \psi_i^*(\mathrm{r})\ \psi_i(\mathrm{r}) + \sum_{i \in val}^{N_{val}} \psi_i^*(\mathrm{r})\ \psi_i(\mathrm{r})$$

$$= n_{core}(\mathrm{r}) + n_{val}(\mathrm{r}) \tag{2-71}$$

for $i \in$ core, $\psi_i = \psi_i^{atom}$, the energy is:

$$E_{KS}[\{\psi_i\}] = \sum_{i}^{occ} \langle \psi_i \left| -\frac{1}{2}\nabla^2 \right| \psi_i \rangle$$

$$+ \int V_{ext}(\mathrm{r})\, n(\mathrm{r})\mathrm{dr} + \frac{1}{2}\int \frac{n(\mathrm{r}_1) n(\mathrm{r}_2)}{|\mathrm{r}_1 - \mathrm{r}_2|} d\mathrm{r}_1 d\mathrm{r}_2 + E_{xc}[n]$$

$$E_{KS}[\{\psi_i\}] = \sum_{i \in core}^{N_{core}} \langle \psi_i \left| -\frac{1}{2}\nabla^2 \right| \psi_i \rangle$$

$$+ \int V_{ext}(\mathrm{r}) n_{core}(\mathrm{r}) \mathrm{dr} + \frac{1}{2} \int \frac{n_{core}(\mathrm{r}_1) n_{core}(\mathrm{r}_2)}{|\mathrm{r}_1 - \mathrm{r}_2|} d\mathrm{r}_1 d\mathrm{r}_2 + E_{xc}[n]$$

$$+ \sum_{i \in val}^{N_{val}} \langle \psi_i \left| -\frac{1}{2}\nabla^2 \right| \psi_i \rangle + \int V_{ext}(\mathrm{r}) n_{val}(\mathrm{r}) \mathrm{dr} + \frac{1}{2} \int \frac{n_{val}(\mathrm{r}_1) n_{val}(\mathrm{r}_2)}{|\mathrm{r}_1 - \mathrm{r}_2|} d\mathrm{r}_1 d\mathrm{r}_2 + E_{xc}[n]$$

$$+ \int \frac{n_{core}(\mathrm{r}_1) n_{val}(\mathrm{r}_2)}{|\mathrm{r}_1 - \mathrm{r}_2|} d\mathrm{r}_1 d\mathrm{r}_2 + E_{xc}[n_{core} + n_{val}] \quad (2\text{-}72)$$

After screening by the core electrons, the potential of the nuclei κ is expressed as:

$$V_{ion,\kappa}(\mathrm{r}) = \frac{Z_\kappa}{|r - R_\kappa|} + \int \frac{n_{core,\,\kappa}(\mathrm{r}_1)}{|\mathrm{r}_1 - \mathrm{r}_2|}\, \mathrm{d}r_1 \quad (2\text{-}73)$$

$$V_{ion,\kappa}(\mathrm{r}) = \frac{Z_{val,\,\kappa}}{|r - R_\kappa|} + \left(-\frac{Z_{core,\,\kappa}}{|r - R_\kappa|} + \int \frac{n_{core,\,\kappa}(\mathrm{r}_1)}{|\mathrm{r}_1 - \mathrm{r}_2|}\, \mathrm{d}r_1 \right) \quad (2\text{-}74)$$

The total energy becomes

$$E = \left(E_{val} + \textstyle\sum_\kappa E_{core,\,\kappa}\right) + \frac{1}{2} \sum_{\substack{(\kappa,\ \kappa') \\ \kappa \neq \kappa'}} \frac{Z_{\mathrm{val},\kappa} Z_{\mathrm{val},\,\kappa'}}{|\mathrm{R}_\kappa - \mathrm{R}_{\kappa'}|} \quad (2\text{-}75)$$

with

$$E_{val,\,KS}[\{\psi_i\}] = \sum_{i \in val}^{N_{val}} \langle \psi_i \left| -\frac{1}{2}\nabla^2 \right| \psi_i \rangle + \int \left(\sum_\kappa V_{ion,\kappa}(r) \right) n_{val}(\mathrm{r}) \mathrm{dr}$$

$$+ \frac{1}{2} \int \frac{n_{val}(\mathrm{r}_1) n_{val}(\mathrm{r}_2)}{|\mathrm{r}_1 - \mathrm{r}_2|} d\mathrm{r}_1 d\mathrm{r}_2 + E_{xc}[n_{core} + n_{val}] \quad (2\text{-}76)$$

where $n_{core} + n_{val}$ is a non-linear exchange energy correlation. According to the previous construction, valence orbitals are orthogonal to core orbitals. Pseudopotentials completely cancel

out the core orbitals from simulation. Therefore, removing core electrons from the equation below:

$$\left(-\frac{1}{2}\nabla^2 + \mathrm{v}\right)|\psi_i \geq \varepsilon_i|\psi_i > \tag{2-77}$$

the result is:

$$\left(-\frac{1}{2}\nabla^2 + \mathrm{v}_{\mathrm{ps}}\right)\left|\psi_{\mathrm{ps},\,i} \geq \varepsilon_{\mathrm{ps},\,i}\right|\psi_{\mathrm{ps},\,i} > \tag{2-78}$$

For the lowest angular momentum channels (s + p…d...f)[53], $\varepsilon_{ps,\,i}$ and $\psi_i\,(\mathrm{r}) = \psi_{\mathrm{ps},\,i}(\mathrm{r})$.

For $\mathrm{r} > \mathrm{r_c}$

$$\int|\psi_i\,(\mathrm{r})|^2\,\mathrm{dr} = \int\left|\psi_{\mathrm{ps},\,i}(\mathrm{r})\right|^2\,\mathrm{dr} \tag{2-79}$$

Specific examples are the popularly used ECP basis for transition metals are the Los Alamos National Laboratory 2 double zeta (LANL2DZ) and non-transition metal systems uses all-electron basis sets. Dunning and coworkers developed the contracted Gaussian type functions, CGTF basis sets such as cc-pVnZ (where n interpolates between 2 and 6). CGTF basis sets like cc-pVDZ, are used to calculate electron correlation in terms of the correlation constant, polarized valence double zeta. Selection of basis set plays a small role in electron density-based approximation methods such as DFT, given to the fact that small basis sets like 6-31G* (DZP) set and Pople basis set are more effective in DFT approximation than a self-consistent correlation basis set of the same size.[56] Modeling of the closed-shell and the open shell systems uses restricted and unrestricted basis sets respectively.

Atomic Units

Researchers in quantum chemistry use a Gaussian-based atomic unit system to write or report their calculated results, to effectively preserve space and time. The term atomic unit is

determined by the operating interactions such as velocities, and forces, acting upon the electron in the ground state of the hydrogen atom. This system is conceived by setting many fundamental constant to unity.[57] For instance, the unit of mass is the mass of the electron (m_e), and $\hbar$ is the unit of angular momentum. The system uses Hartree (E_h) as the atomic energy unit $\left(\frac{e^2}{a_0}\right)$.

$$E_h = \frac{e^2}{4\pi\,\varepsilon_0\,a_0} = 27.211\ eV \tag{2-80}$$

where the atomic unit of length is Bohr's radius and is given by:

$$a_0 = \frac{\hbar^2}{m_e\,e^2} = 0.5291177\ \text{Å} \tag{2-81}$$

CHAPTER 3

COMPUTATIONAL DETAILS

All geometry optimizations were performed using NWChem 6.5[60] on a Linux-based computer cluster using HF[61,62] and DFT/B3LYP[63,64] levels of theory with the LANL2DZ ECP[65] basis set for Rh, and the LANL2DZ ECP, cc-pVDZ[66] and cc-pVTZ[66] basis sets for all other atoms for the parent complexes. The nitrile-ligated complexes were calculated using LANL2DZ ECP for Rh and cc-pVDZ for all other atoms. ECCE 7.0 was used to create and manage the calculations.[67] All geometry optimizations were performed with initially C_1 symmetry (that is, without any assumed symmetry leading to geometry restrictions). The HF and DFT results were calculated independently of each other.

Discussion of Results

Recent experimental work in Dr. Cassandra Eagle's research group has indicated that there are significant differences in the isomeric ratios obtained among the possible products when synthesizing those carboxylamidate complexes (shown in Figure 1) and that the crystal structures for some of the $Rh_2(NHCOR)_4NCR$ complexes exhibit anomalous Rh-N-C bond angles.[58,68] For example, the Rh-N-C bond angle of 2 equivalent complexes of ortho-tolunitrile was larger (173.4(3)°) than their corresponding 1 equivalent complexes of ortho-tolunitrile (162.5(3)°), and the Rh-N-C bond angle of 1 equivalent complexes of meta-tolunitrile was smaller (162.7(5)°) than (164.5(5)°) in 2 equivalent complexes of meta-tolunitrile.[68]

Ab initio calculations have been undertaken of the experimental complexes, $Rh_2(NPhCOCH_3)_4(NCC_6H_4CH_3)_2$, in an attempt to gain further insight into the details of the bonding. The crystal-packing is referring to how each molecule arranged in crystal structure. Thus, it mainly uses to interpret the crystallography. These calculations obtained similar Rh-N-C

bond angles[59] reducing the probability that crystal-packing forces could explain the crystallography. However, the size of these complexes makes detailed computational study in these complexes impractical, necessitating the use of a simplified model structure to possibly explain the unexpected Rh-N-C bond angles observed in the crystal structures.

First, the calculations were performed for dirhodium complexes that coordinate only to equatorial ligands. Theses equatorial ligands were formate, acetate, formamide, and acetamide. The structures of theses ligands are shown in Figure 6.

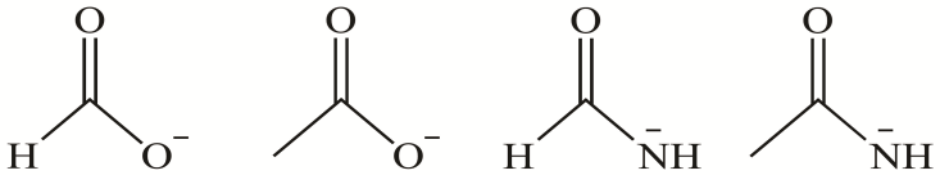

Figure 6: Structures of formate, acetate, formamide, and acetamide.

For the $Rh_2(NHCOH)_4$ isomers, the 2,2-cis has the lowest energy (see Table 1), followed by 2,2-trans, 3,1-, and 4,0-, which correlates with the fractional abundance obtained during synthesis.[57] This order of relative energies is maintained after the addition of either an NC^- or NCH ligand to the axial site of one of the rhodium atoms (see Tables 2 and 3). Since the axial ligand could coordinate to the parent ligand from two sides. Coordination to the nitrogen side is more stable (N-side in the table) for the 3,1- and 4,0- isomers and is favored for both NC^- and NCH. On the other hand, for NC^-, coordination by the carbon is more stable (labeled C-side in Table 2) for the formate and acetate forms. Since these systems are models for carbene catalytic processes, coordination by carbon is not surprising.

Table 1: Total energies for the Rh_2L_4 complexes

Ligand	**Isomer**	**Basis Set(s)***	**HF Energy** (E_h)	**DFT/B3LYP,Energy** (E_h)
Formate		L	-970.010593759474	-975.640373843995
		LD	-970.267008248122	-975.879893398776
		LT	-970.488849768195	-976.112980691106
Acetate		L	-1126.166712246929	-1133.027791361317
		LD	-1126.469289946561	-1133.185472846297
		LT	-1126.731021214322	-1133.472734098233
Formamide	2,2-cis	L	-890.674895603972	-896.259314139918
		LD	-890.897577498157	-896.378960871760
		LT	-891.095034322822	-896.594410314401
	2,2-trans	L	-890.676537546521	-896.258959535657
		LD	-890.897789377086	-896.377557659750
		LT	-891.094782241035	-896.592470895792
	3.1-	L	-890.673505502568	-896.257077739938
		LD	-890.896233598173	-896.377032098842
		LT	-891.093537067149	-896.592254199788

	4,0-	L	-890.667689427883	-896.250825438755
		LD	-890.891985550565	-896.372705124347
		LT	-891.089262345502	-896.587780682981
Acetamide	2,2-cis	L	-1046.814886926344	-1053.531953635089
		LD	-1047.087682884435	-1053.672925869690
		LT	-1047.325977203864	-1053.943145240620
	2,2-trans	L	-1046.814800123630	-1053.53004536379
		LD	-1047.087686548909	-1053.671233983537
		LT		-1053.94095438433
	3,1-	L	-1046.813548787117	-1053.529713374218
		LD	-1047.086435012249	-1053.671233983537
		LT	-1047.324517778192	-1053.940987893251
	4,0-	L	-1046.808323152244	-1053.523970987776
		LD	-1047.083678317213	-1053.667081594230
		LT		-1053.936855116669

Note: *L - LANL2DZ ECP

LD - LANL2DZ ECP, cc-pVDZ

LT - LANL2DZ ECP, cc-pVTZ

Table 2: Total energies and Rh-N-C bond angle for the Rh_2L_4NC complexes

Ligand	Isomer	HF/LANL2DZ ECP, cc-pVDZ		DFT/B3LYP/ LANL2DZECP,cc-pVDZ	
		HF Energy (E_h)	Bond Angle (degrees)	DFT Energy (E_h)	Bond Angle (degrees)
Formate		-1062.65298732856	180.0	-1068.807254260231	180.0
	C side	-1062.66779762924	180.0	-1068.824976049848	180.0
Acetate		-1218.84638002778	180.0	-1226.102836096669	180.0
	C side	-1218.86031951289	179.9	-1226.119599348368	179.8
Formamide	2,2-cis	-983.27433269643	174.4	-989.301187893840	170.7
	2,2-trans	-983.27188118796	180.0	-989.296255464163	179.7
	3,1-	-983.26325722619	176.0	-989.290745994772	173.4
	3,1- (N side)	-983.28028903729	176.4	-989.304615163271	173.3
	4,0-	-983.24924815312	179.9	-989.277985445145	180.0
	4,0- (N side)	-983.28368888921	179.5	-989.306035293427	180.0

Acetamide	2,2-cis	-1139.45865242987	174.6	-1146.58903813891	170.2
	2,2-trans	-1139.45619814251	179.8	-1146.58399724631	179.9
	3,1-	-1139.44790095675	175.7	-1146.57871351425	172.5
	3,1- (N side)	-1139.46464104049	176.2	-1146.59257076079	173.0
	4,0-	-1139.43458706783	180.0	-1146.56628473465	180.0
	4,0- (N side)	-1139.46841659213	179.9	-1146.59433314283	179.0

Table 3: Total energies and Rh-N-C bond angle for the Rh_2L_4NCH complexes

Ligand	Isomer	HF/LANL2DZ ECP, cc-pVDZ		DFT/B3LYP/LANL2DZ ECP, cc-pVDZ	
		HF Energy (E_h)	Bond Angle (degrees)	DFT Energy (E_h)	Bond Angle (degrees)
Formate		-1063.1703450709	180.0	-1069.332828341823	180.0
Acetate		-1219.3696699757	180.0	-1226.635337706707	179.8
Formamide	2,2-cis	-983.795922604410	169.1	-989.829323561224	172.6
	2,2-trans	-983.795497838816	179.7	-989.827254379789	179.3
	3,1-	-983.793955303956	172.0	-983.793955303956	172.0
	3,1- (N side)	-983.794523997672	168.5	-989.827158665812	174.6
	4,0-	-983.789076252332	179.8	-989.822393398403	179.9
	4,0- (N side)	-983.790383691276	179.8	-989.822609254377	178.4
Acetamide	2,2-cis	-1139.98407071468	168.0	-1147.121450388207	172.6
	2,2-trans	-1139.98351586836	178.8	-1147.119183386391	179.9
	3,1-	-1139.98214927811	172.1	-1147.119070905657	175.3

	3,1- (N side)	-1139.98294716252	172.1	-1147.119484868305	175.1
	4,0-	-1139.97768366316	180.0	-1147.114685314343	180.0
	4,0- (N side)	-1139.97933153977	179.6	-1147.115516513339	179.9

The HOMO-1 and HOMO-2 molecular orbitals are nearly identical in energy and rotated 90^{o} with respect to each other (Figure 7 shows one of these orbitals) for $Rh_2(CO_2H)_4NC^-$. These MO's also show characteristic features consistent with "π-back bonding." In each one, there is significant involvement of a d orbital from the rhodium and one of the π MO's from the cyanide. In contrast, for $Rh_2(CO_2H)_4NCH$ the comparable MO's do not show any involvement of NCH (see Figure 7).

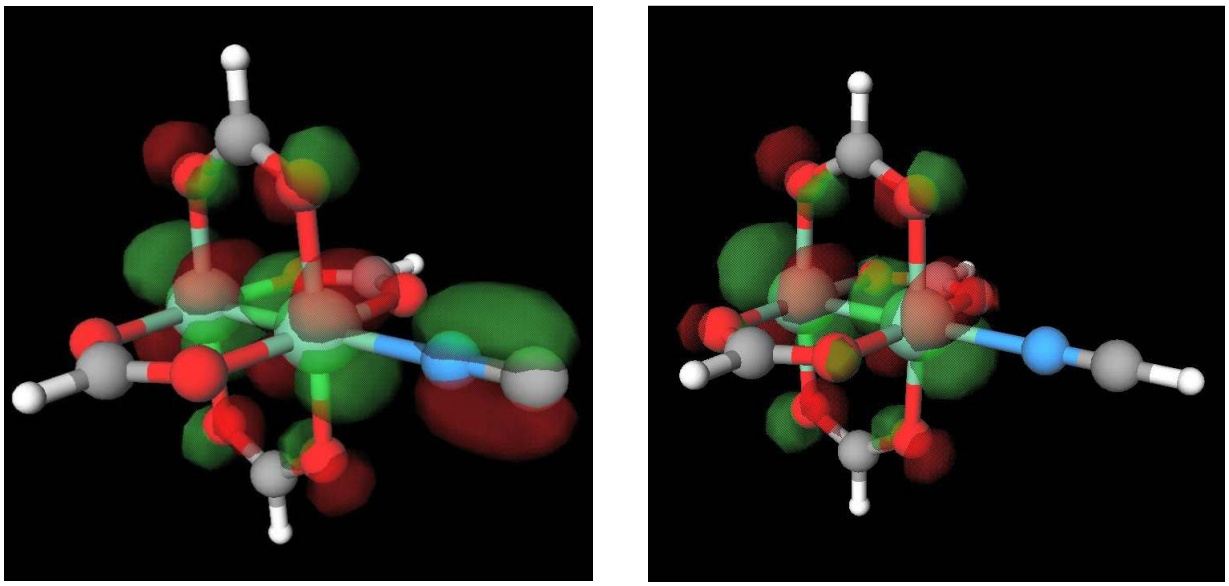

a **b**

Figure 7: Molecular orbital pictures for the HOMO-1 for $Rh_2(CO_2H)_4NC^-$ and $Rh_2(CO_2H)_4NCH$

For $Rh_2(NHCOH)_4NC^-$ similar features are observed, except when the Rh-N-C bond angle decreases from 180°, only one of these "back bonding" MO's is observed in the calculations. Again, for NCH, there is no evidence for "back bonding." With only one, or no "back bonds," the Rh-N-C bond angle is not fixed at 180°, and is free to decrease as the complex minimizes its energy. Interestingly, as may be seen in Figure 8, the tilt is towards the nitrogens for NC^-, but towards the oxygens for NCH.

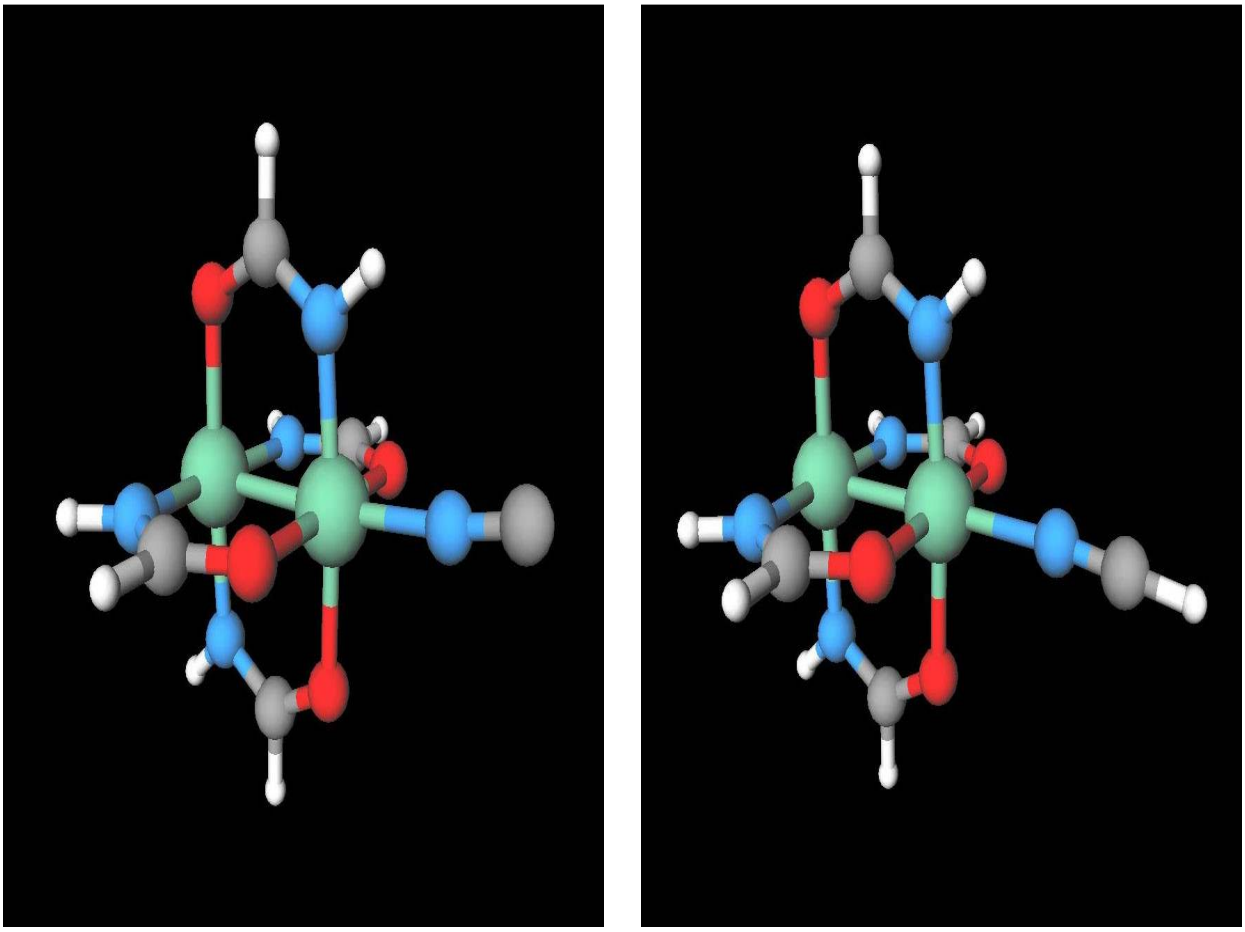

a b

Figure 8: Structures of 3,1- $Rh_2(NHCOH)_4NC$ and $Rh_2(NHCOH)_4NCH$ illustrating the tilt of the axial ligand to the nitrogens for NC^- and to the oxygens for NCH

Seemingly minor effects, such as switching the ligand from NC^- to NCH, may alter the bonding in the dirhodium complexes. It is also important to remember that successful bonding

requires not only the correct geometry for overlap, but also comparable energies. Even minor changes can cause orbital energies to shift sufficiently to cause observable changes in structure. In addition, analysis of data obtained from the geometry optimization and single-point energy calculations performed using HF level of theory will help explain the relative stabilities of dirhodium complexes.

Table 4: Total energies and energy differences from RHF/LANL2DZ, cc-pVDZ calculations for the dirhodium complexes (acetate ligand); 1 Hartree = 2625.5 kJ/mol

Complexes	Energies (Hartree)	ΔE_1 (Hartree)	ΔE_1 (kJ/mol)
(ACO)	-227.24323	----------	----------
$Rh_2(ACO)$	-444.5627	217.31947	570572.27
$Rh_2(ACO)_2$	-666.8723	222.3109	583673.85
$Rh_2(ACO)_3$	-898.8725	232.0002	609116.53
$Rh_2(ACO)_4$	-1126.4693	227.5968	597555.4

Table 5: Total energies and energy differences from RHF/LANL2DZ, cc-pVDZ calculations for the dirhodium complexes (acetamide ligand); 1 Hartree = 2625.5 kJ/mol

Complexes	Energies (Hartree)	ΔE_2 (Hartree)	ΔE_2 (kJ/mol)
($NHCOCH_3$)	-207.3803	----------	----------
$Rh_2(NHCOCH_3)$	-424.7225	217.3422	570631.95

$Rh_2(NHCOCH_3)_2$	-688.3266	263.6041	692092.6
$Rh_2(NHCOCH_3)_3$	-844.1322	155.8056	409067.6
$Rh_2(NHCOCH_3)_4$	-1047.1275	202.9954	532964.4

Table 6: Total energies and energy differences from RHF/LANL2DZ, cc-pVDZ calculations for the dirhodium complexes (with formate); 1 Hartree = 2625.5 kJ/mol

Complexes	Energies (Hartree)	ΔE_3 (Hartree)	ΔE_3 (kJ/mol)
(OCHO)	-188.19623	----------	----------
$Rh_2(OCHO)$	-405.51901	217.3228	570580.93
$Rh_2(OCHO)_2$	-599.45410	193.9351	509176.58
$Rh_2(OCHO)_3$	-807.31151	207.85741	545729.63
$Rh_2(OCHO)_4$	-970.26711	162.9556	427839.93

Interpreting the relationship between stability and energy is fundamental to successfully discuss the relative stabilities of the complexes. A system in its lowest energy is considered to be chemically stable (thermodynamically stable). That is the lower the energy, the higher the

stability of the system and vice versa. The data available from dirhodium complexes showed that $Rh_2(ACO)_4$ has the lowest energies making it the most stable, whereas $Rh_2(OCHO)$ had the highest energies and as a results the least stable. Moreover, the calculated energies also show a considerable decrease in energy as the size of the substituent increases.

.

Pictorial representations of dirhodium complexes shows the dirhodium with four acetate ligands (Figure 9), with four acetamide ligands (Figure 10), and with four formate ligands (Figure 11).

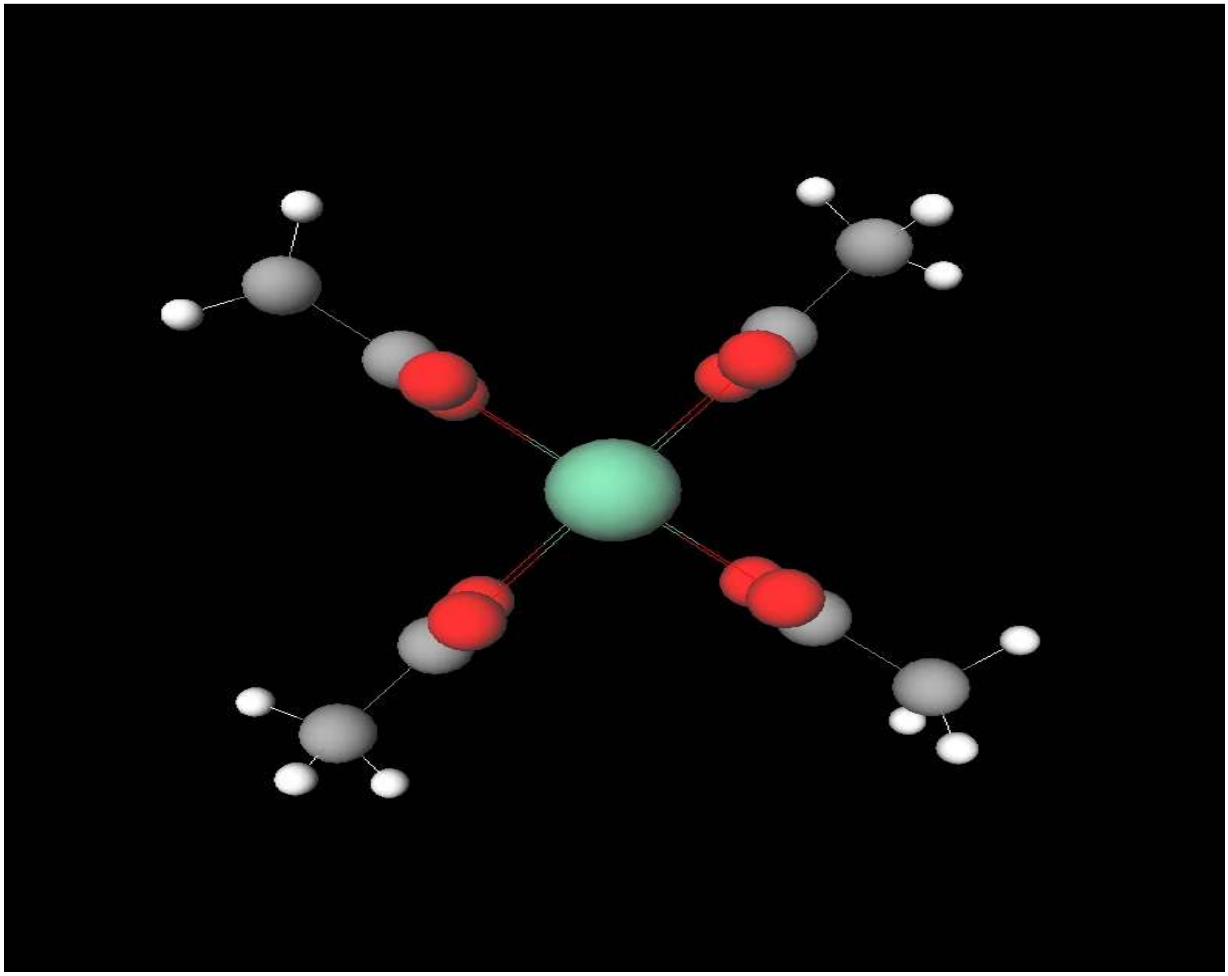

Figure 9: Eccé® pictorial representations of $Rh_2(ACO)_4$

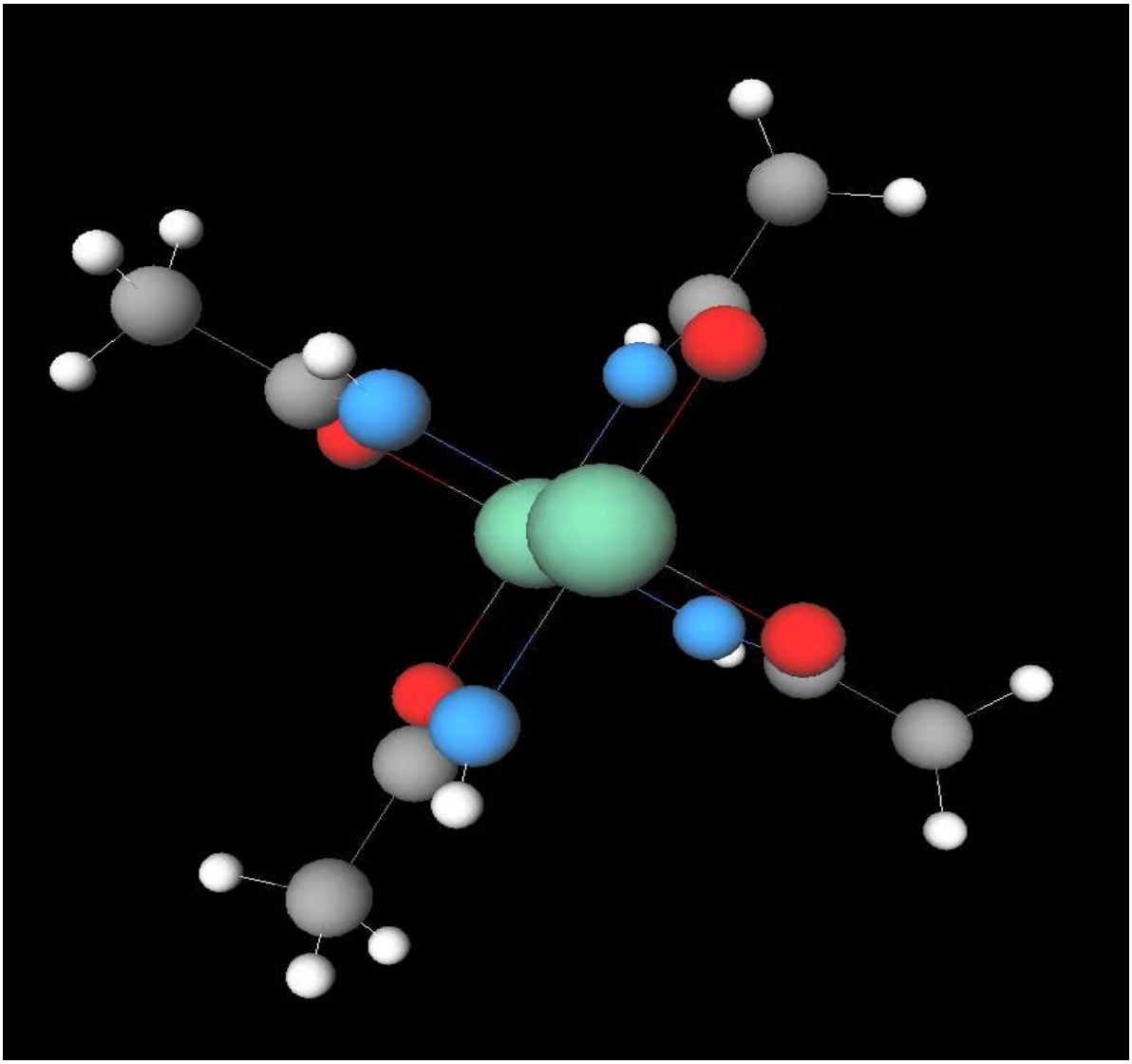

Figure 10: Eccé® pictorial representations of $Rh_2(NHCOCH_3)_4$

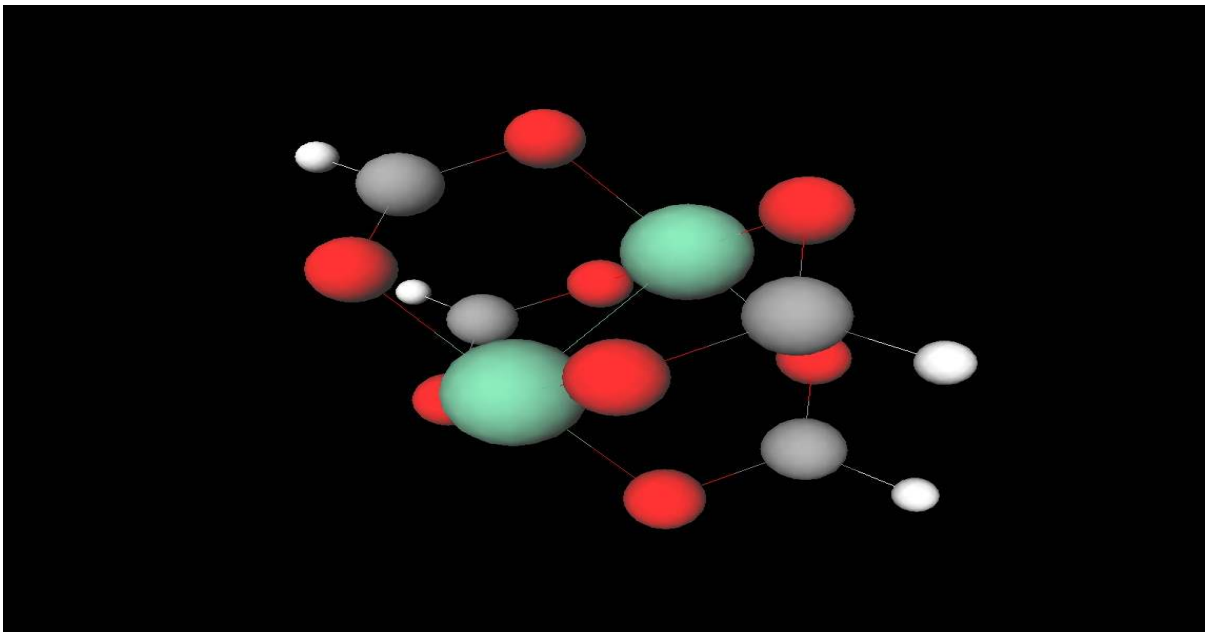

Figure 11: Eccé® pictorial representations of $Rh_2(OCHO)_4$

Also, analysis of data obtained from the geometry optimization and single-point energy calculations performed using HF level of theory will help explaining the relative stabilities of cyanoligated rhodium dimer complexes.

Table 7: Total energies from RHF/LANL2DZ, cc-pVDZ calculations for the (Rh-NC-CH_3); 1 Hartree = 2625.5 kJ/mol

Ligand	Isomer	Complexes	Total Energies (Hartree)
Acetate		$Rh_2(ACO)(CH_3CN)$	-576.5407794414
		$Rh_2(ACO)_2(CH_3CN)$	-803.1826509803
		$Rh_2(ACO)_3(CH_3CN)$	-1030.863989213
		$Rh_2(ACO)_4(CH_3CN)$	-1258.427807917

Acetamide	2.2-cis	$Rh_2(NHCOCH_3)$ (CH_3CN)	-556.6926115914
		$Rh_2(NHCOCH_3)_2$ (CH_3CN)	-763.5486902378
		$Rh_2(NHCOCH_3)_3(CH_3CN)$	-971.5981542873
		$Rh_2(NHCOCH_3)_4(CH_3CN)$	-1179.041821458
Formate		$Rh_2(OCHO)$ (CH_3CN)	-537.4927963902
		$Rh_2(OCHO)_2$ (CH_3CN)	-724.9985094401
		$Rh_2(OCHO)_3$ (CH_3CN)	-913.8087836014
		$Rh_2(OCHO)_4$ (CH_3CN)	-1102.272284258

The table above proves that the energy decreases as the number of ligands increases. It means that when the complex binds with four ligands, it will have the lowest energy. Since there is an inverse relationship between energy and stability, complexes contain four ligands have the highest stability and the lowest energy. Thus, the order of stabilities of Rh-NC-CH_3 (acetate ligand) complexes is as follows:

$Rh_2(ACO)_4(CH_3CN)>Rh_2(ACO)_3(CH_3CN)>Rh_2(ACO)_2(CH_3CN)>Rh_2(ACO)(CH_3CN)$.

The order of stabilities of Rh-NC-CH_3 (acetamide ligand) complexes is as follows:

$Rh_2(NHCOCH_3)_4(CH_3CN)>Rh_2(NHCOCH_3)_3(CH_3CN)>Rh_2(NHCOCH_3)_2(CH_3CN)>Rh_2(NHCOCH_3)(CH_3CN)$.

And the order of stabilities of Rh-NC-CH_3 (formate ligand) complexes is as follows:

$Rh_2(OCHO)_4$ (CH_3CN)>$Rh_2(OCHO)_3$ (CH_3CN)>$Rh_2(OCHO)_2$ (CH_3CN)>$Rh_2(OCHO)$ (CH_3CN)

By using the same method of calculation, the total energies of Rh-NC-C_6H_5 complexes were calculated. These calculations then were used to demonstrate the stability of different complexes.

Table 8: Total energies from RHF/LANL2DZ, cc-pVDZ calculations for the (Rh-NC-C_6H_5); 1 Hartree = 2625.5 kJ/mol

Ligand	Isomer	Complexes	Total Energies (Hartree)
Acetate		$Rh_2(ACO)(C_6H_5CN)$	-767.0534640401
		$Rh_2(ACO)_2(C_6H_5CN)$	-993.7199652252
		$Rh_2(ACO)_3(C_6H_5CN)$	-1221.392799923
		$Rh_2(ACO)_4(C_6H_5CN)$	-1448.952816916
Acetamide	2,2-cis	$Rh_2(NHCOCH_3)$ (C_6H_5CN)	-747.203557028
		$Rh_2(NHCOCH_3)_2(C_6H_5CN)$	-954.085318949
		$Rh_2(NHCOCH_3)_3(C_6H_5CN)$	-1160.10458783
		$Rh_2(NHCOCH_3)_4(C_6H_5CN)$	-1369.56659546

Formate		$Rh_2(OCHO)(C_6H_5CN)$	-728.017897339
		$Rh_2(OCHO)_2(C_6H_5CN)$	-915.538746953
		$Rh_2(OCHO)_3(C_6H_5CN)$	-1104.34074079
		$Rh_2(OCHO)_4(C_6H_5CN)$	-1292.80126912

The data available from Table 8 show that $Rh_2(ACO)_4(C_6H_5CN)$ has the lowest energy making it the most stable complex. The $Rh_2(OCHO)(C_6H_5CN)$ complex had the highest energy and, as a result, it is the least stable complex. From Table 8, the stability of (Rh-NC-C_6H_5) complexes with acetate, acetamide, and formate ligands is as follows:

$Rh_2(ACO)_4(C_6H_5CN)$> $Rh_2(NHCOCH_3)_4(C_6H_5CN)$> $Rh_2(OCHO)_4(C_6H_5CN)$>

$Rh_2(ACO)_3(C_6H_5CN)$> $Rh_2(NHCOCH_3)_3(C_6H_5CN)$> $Rh_2(OCHO)_3(C_6H_5CN)$>

$Rh_2(ACO)_2(C_6H_5CN)$> $Rh_2(NHCOCH_3)_2(C_6H_5CN)$> $Rh_2(OCHO)_2(C_6H_5CN)$>

$Rh_2(ACO)(C_6H_5CN)$> $Rh_2(NHCOCH_3)$ (C_6H_5CN)> $Rh_2(OCHO)(C_6H_5CN)$.

The above trend is an indication of the difficulty in synthesizing the $Rh_2(OCHO)(C_6H_5CN)$, the $Rh_2(NHCOCH_3)$ (C_6H_5CN), and the $Rh_2(ACO)(C_6H_5CN)$ complexes. It also explains why the $Rh_2(ACO)_4(C_6H_5CN)$, the $Rh_2(NHCOCH_3)_4(C_6H_5CN)$, and the $Rh_2(OCHO)_4(C_6H_5CN)$ complexes are the easiest to synthesize (because of having the lowest energy). Therefore, the complexes with the lowest energies are easier to be synthesized than those having highest energies. The calculated energies also show a significant decrease in energy as the size of the substituent increases.

CHAPTER 4

CONCLUSIONS

From the data available from the DFT and HF calculations for the $Rh_2(NHCOH)_4$ isomers, the 2,2-cis has the lowest energy, followed by 2,2-trans, 3,1-, and 4,0-. which correlates with the fractional abundance obtained during synthesis. This order of relative energies is maintained after the addition of either a NC^- or NCH ligand to the axial site of one of the rhodium atoms.

A small effect that might occur, like switching the ligand from NC^- to NCH, can change the bonding in the dirhodium complexes. It is also important to remember that successful bonding requires not only the correct geometry for overlap, but also comparable energies. Even minor changes can cause orbital energies to shift sufficiently to cause observable changes in structure.

Knowing the relationship between the energies and stability allows us to discuss and explain the relative stabilities of the complexes. The complex with the lowest energy will be the highest in stability, and it is said to be thermodynamically stable, and the complex with the highest energy, will be the least stability and more difficult to be synthesized. The complexes binding with larger number of ligands will have lower energy. Thus, Tables 4, 5, and 6 show that the complexes bound with four ligands have lower energy than those bound with three, two, and one ligand.

REFERENCES

1. Redhu, S., Anil, J. Molecular modelling: a new scaffold for drug design. I*nt. J. Pharm. Pharm*. *Sci*. **2013**, *5*, 6-7.
2. Cohen, N.; Blaney, J.; Humblet, C.; Gund, P.; Barry, D. Molecular Modeling Software And Methods For Medicinal Chemistry. *J. Med. Chem*. **1990**, *33*, 883-894.
3. Dykstra, C.; Frenking, G.; Kim, K.; Scuseria, G.; Eds. *Theory and applications of computational chemistry: the first forty years*. Elsevier, **2011**.
4. Labanowski, J. K., Andzelm, J. W., Eds. *Density functional methods in chemistry*. Springer Science & Business Media, **2012**.
5. Fu, P. K. L., Bradley, P. M., & Turro, C. DNA cleavage by photogenerated $Rh_2(O_2CCH_3)_4(H_2O)^{2+}$. *Inorg. Chem.* **2011,** *40*, 2476-2477.
6. Remko, M. *Molecular Modeling. Principles and Applications*. SAP–Slovak Academic Press: Bratislava, **2000**, 240.
7. Hancock, R. D. Molecular mechanics calculations and metal ion recognition. *Acc. Chem. Res.* **1990**, *23,* 253-257.
8. Sun, Y.; Anderson, C. J.; Pajeau, T. S.; Reichert, D. E.; Hancock, R. D.; Motekaitis, R. J. Welch, M. J. Indium (III) and gallium (III) complexes of bis (aminoethanethiol) ligands with different denticities: stabilities, molecular modeling, and in vivo behavior. *J. Med Chem.* **1996,** *39,* 458-470.
9. Cambridge Crystallographic Data Centre, Cambridge England.
10. Thöm, V. J.; Fox, C. C.; Boeyens, J. C. A.; Hancock, R. D. Molecular mechanics and crystallography study of hole sizes in nitrogen-donor tetraaza macrocycles. *J. Am.*

Chem. Soc. **1984**, *106*, 5947-5955.

11. Hancock, R. D. Macrocycles and their selectivity for metal ions on the basis of size. *Pure Appl. Chem*. **1986**, *58*, 1445-1452.
12. Hancock, R. D. Molecular mechanics calculations as a tool in coordination chemistry. *Prog. Inorg. Chem.* **1989,** *37*, 187-291.
13. Lin, X.; Xi, Y.; Sun, J. A computational study on the competing intramolecular amidation and aziridination reactions catalyzed by dirhodium tetracarboxylate. *Comput. Theor. Chem.* **2012,** *999,* 74-82.
14. Li, L.; Li, M.; Wang, X.; Wang, Q. Density functional theory study on the molecular taekwondo process of pyrene-armed calix [4] azacrowns. *Comput. Theor. Chem.* **2014,** *1031*, 40-49.
15. Roothaan, C. C. J. New developments in molecular orbital theory" *Rev. Mod. Phys.* **1951**, *23*, 69.
16. Hall, G. G. The molecular orbital theory of chemical valency. VIII. A method of calculating ionization potentials. *Proc. R. Soc. Lond.* **1951**, *A 205*, 541.
17. Boys, S. F. Electronic wave functions. II. A calculation for the ground state of the beryllium atom. *Proc. R. Soc. Lond.* **1950**, *A 200*, 542.
18. Kurt, M.; Yurdakul, Ş. Molecular structure and vibrational spectra of 1, 2-bis (4-pyridyl) ethane by density functional theory and ab initio Hartree-Fock calculations. *J. Mol. Struct.* **2003,** *654,* 1-9.
19. Ricca, A.; Bauschlicher Jr.; C. W. Successive H_2O binding energies for Fe (H_2O) N^+. *J. Phys. Chem.* **1995**, *99,* 9003-9007.

20. Bauschlicher Jr, C. W., Partridge, H. A modification of the Gaussian□2 approach using density functional theory. *J. Phys. Chem.* **1995**, 103, 1788-1791.

21. Doyle, M. P. Perspective on dirhodium carboxamidates as catalysts. *J. Org. Chem.* **2006**, *71*, 9253-9260.

22. Doyle, M. P.; John, T. C. Synthesis of dirhodium (II) tetrakis [methyl 1-(3-phenylpropanoyl)-2-oxaimidazolidine-4 (S)-carboxylate], Rh 2 (4S-MPPIM) 4. *Tetrahedron: Asymmetry.* **2003,** *14,* 3601-3604.

23. Cotton, F. A.; Murillo, C. A.; Walton, R. A., *Multiple bonds between metal atoms*. 3rd ed.; Springer Science & Business Media Inc.: **2005**, 465.

24. Quarshie, Fredricka Francisca. Synthesis and Characterization of 2, 2-cis- [$Rh_2(NPhCOCH_3)_4$] • NCC_6H_4R, East Tennessee State University, Master's Thesis, **2013**.

25. Adekunle, F. A. O.; Semire, B.; Odunola, O. A. Synthesis, characterization and semi-empirical study of Di-nuclear mixed-ligands complexes of Ru (II). *Orient J. chem*. **2013**, *29*, 945-951.

26. Fehlhammer, W. P., Fritz, M. Emergence of a CNH and cyano complex based organometallic chemistry. *Chem. Rev.* **1993**, *93,* 1243-1280.

27. Tambe, N. A, Synthesis and Characterization of Three New Tetrakis (N-phenyl acetamidato) Dirhodium(II) Nitrile Complexes, East Tennessee State University, Master's Thesis, **2013.**

28. Busch, P.; Heinonen, T.; Lahti, P. Heisenberg's uncertainty principle. *Phys. Rep*. **2007,** *452,* 155-176.

29. Debrah, Duke A. Molecular Modeling of Dirhodium Complexes. East Tennessee State University, Master's Thesis, **2014**.

30. Schrodinger, E. *Ann. Phys.* **1926**, *80*, 437-490.

31. Schrodinger, E. *Ann. Phys.* **1926**, *81*, 109-139.

32. Born, M. Quantum mechanics of impact processes. *J. Phys*. **1926**, *38,* 803-827.

33. Griffiths, D. *Introduction to Quantum Mechanics* 2nd ed; Pearson Education Inc.: **2005,** 183-184.

34. Pauli, W. On the connexion between the completion of electron groups in an atom with the complex structure of spectra. *Zeit. Phys*. **1925**, *31,* 765.

35. Wilson, S. *Electron correlation in molecules*. Courier Corporation, **2014**.

36. Sherrill, C. D. An introduction to Hartree-Fock molecular orbital theory. *School of Chemistry and Biochemistry Georgia Institute of Technology.* **2000**.

37. Parr, R. G. Density functional theory of atoms and molecules. *Horizons of Quantum Chemistry*. Springer Netherlands. **1980**, 5-15.

38. Levine, I. N. *Quantum chemistry*. 7th ed.; Pearson Education Inc.: **2014**, 409-411

39. Roothaan, C. C. J. New developments in molecular orbital theory. *Rev. Mod. Phys*. **1951**, *23*, 69.

40. Kümmel, H. G. A biography of the coupled cluster method. In Bishop, R. F.; Brandes, T.; Gernoth, K. A.; Walet, N. R.; Xian, Y. *Recent progress in many-body theories Proceedings of the 11th international conference.* World Scientific Publishing: Singapore, **2002**, 334–348.

41. Cramer, C. J. *Essentials of Computational Chemistry*. John Wiley & Sons, Ltd: Chichester, **2002**, 191–232.

42. Shavitt, I; Bartlett, R. J. *Many-Body Methods in Chemistry and Physics: MBPT and Coupled-Cluster Theory*. Cambridge University Press. **2009**.

43. Burke, K. The ABC of DFT, 2007. Burke Research Group. *http://chem. ps. uci. edu/kieron/dft 36*. (accessed Feb 14, 2016).

44. Lieb, E. H. Some problems in statistical mechanics that I would like to see solved. *Physica A*. **1999**, *263*, 491-499.

45. Jánosfalvi, Z.; Sen, K.; Nagy, A. Cusp conditions for non-interacting kinetic energy density of the density functional theory. *Phys. Lett A.* **2005**, *344,* 1-6.

46. Kohn, W., Sham, L. J. Self-consistent equations including exchange and correlation effects. *Phys. Rev*. **1965**, *140*, A1133.

47. Levine, I. N. *Quantum Chemistry*.7th ed.; Pearson Education Inc.: **2014,** 559.

48. Levine, I. N. *Quantum Chemistry*.7th ed.; Pearson Education Inc.: **2014,** 560.

49. Seidl, A., Görling, A., Vogl, P., Majewski, J. A., Levy, M. Generalized Kohn-Sham schemes and the band-gap problem. *Phys. Rev B*. **1996**, *53*, 3764.

50. Young, D. C. *Computational Chemistry: A Practical Guide for Applying Techniques to Real World Problem;* John Wiley & Sons Inc.: **2001,** 45.

51. Kohn, W.; Becke, A. D.; Parr, R. G. Density functional theory of electronic structure. *J Phys. Chem.* **1996**, *100,* 12974-12980.

52. Boys, S. F. Electronic wave functions. I. A general method of calculation for the stationary states of any molecular system. *Proc Math Phys Eng Sci*. **1950**, *200*, 1063.

53. Papajak, E., Zheng, J., Xu, X., Leverentz, H. R., Truhlar, D. G. Perspectives on basis sets beautiful: seasonal plantings of diffuse basis functions. *J. Chem. Theory Comput.* **2011**, *7*, 3027-3034.

54. Krauss, M., Stevens, W. J. Effective potentials in molecular quantum chemistry. *Ann. Rev. Phys Chem*. **1984**, *35*, 357-385.

55. Hamann, D. R..; Schlüter, M.; Chiang, C. Norm-conserving pseudopotentials. *Phys. Rev.* **1979**, *43,* 1494.

56. Boese, A. D.; Martin, J. M.; Handy, N. C. The role of the basis set: Assessing density functional theory. *J. Chem. Phys.* **2003**, *119,* 3005-3014.

57. Shull, H.; Hall, G.G. Atomic units. *Nature*. **1959**, *184*, 1559-1560.

58. Harris, C. K., Synthesis and Characterization of Five New Tetrakis(N-phenylacetamidato) Dirhodium(II) Amine Complexes and One Molybdenum Cofactor Described Crystallographically, East Tennessee State University, Master's Thesis, **2015**.

59. Debrah, D. A., Molecular Modeling of Dirhodium Complexes, East Tennessee State University, Master's Thesis, **2014**.

60. Valiev, M., Bylaska, E.J., Govind, N., Kowalski, K., Straatsma, T. P., van Dam, H. J. J., Wang, D., Nieplocha, J., Apra, E., Windus, T. L., de Jong, W. A., NWChem: a comprehensive and scalable open-source solution for large scale molecular simulations. *Comput. Phys. Commun*. **2010**, *181*, 1477.

61. Hartree, D. R. The wave mechanics of an atom with a non-Coulomb central field. Part I. Theory and methods. *Proc. Cambridge Phil*. Soc. **1928**, *24*, 426.

62. Fock, V. Z. *Phys*. **1930**, *61*, 126.

63. Hohenberg, P., Kohn. W., Inhomogeneous electron gas., *Phys*. Rev. **1964**, *136*, B864.

64. Becke, A. D. A new mixing of Hartree–Fock and local density□functional theories. *J. Chem. Phys.* **1993**, *98*, 1372-1377.

65. Hay, P. J., Wadt, W. R., Ab initio effective core potentials for molecular calculations. Potentials for the transition metal atoms Sc to Hg. *J. Chem. Phys.* **1985**, *82*, 270-283.

66. Dunning, Jr., T.H. J. Gaussian basis sets for use in correlated molecular calculations. I. The atoms boron through neon and hydrogen. *Chem. Phys*. **1989**, *90*, 1007.

67. Black, G.D., Schuchardt, K.L., Gracio, D.K., Palmer, B., In Computational Science - ICCS 2003, *International Conference Saint Petersburg Russian Federation, Melbourne, Australia*. **2003**, *2660*, 122-131.

68. Quarshie, F, F., Synthesis and Characterization of 2,2-cis-[Rh2(NPhCOCH3)4] •NCC6H4R, East Tennessee State University, Master's Thesis, **2013**.

VITA

YAZEED ASIRI

Education:	M.S. Chemistry, East Tennessee State University (ETSU), Johnson City, Tennessee 2017.
	B.Sc. Chemistry, Taif University, Kingdom of Saudi Arabia, 2007-2011.
Professional Experience:	Teaching Assistant, Department of Chemistry, Faculty of Science, Taif University from 16/08/2011.
Research Experience:	Ceramic and Metal Matrix Composites as Oxidation Protection of Titanium Aluminide using Glass-Ceramic Coating. (Taif University, Kingdom of Saudi Arabia)
	Ab Initio and Semi-Empirical Calculations of Cyanoligated Rhodium Dimer Complexes. (East Tennessee State University Johnson City, TN, USA)
Publications:	**Asiri, Yazeed M.;** Kirkby, Scott J. Hartree-Fock and Density Functional Theory Calculations of Nitrile Ligated Dirhodium Complexes, 68th Southeast Regional Meeting of the American Chemical Society, Columbia, South Carolina, United States, 23-26 October 2016 (2016), SERMACS-109, American Chemical Society, Washington, D.C.)
	Asiri, Yazeed; **Kirkby, Scott J.** *Ab Initio* and Semi-Empirical Calculations of Cyanoligated Rhodium Dimer Complexes, 47th Central Regional Meeting of the American Chemical Society,

Covington, Kentucky, United States, 18-21 May 2016 (2016), CERM-224, American Chemical Society, Washington, D.C.)

Asiri, Yazeed; Kirkby, Scott J. *Ab Initio* and Semi-Empirical Calculations of Cyanoligated Rhodium Dimer Complexes, 2016 Appalachian Student Research Forum, Johnson City, Tennessee, 6-7 April 2016, Abstract 93.